PHYSICAL REVIEW D **81,** 074032 (2010)

Nonrelativistic QCD predictions of D-wave quarkonia ${}^3D_J(J = 1, 2, 3)$ decay into light hadrons at order α_s^3

Zhi-Guo He,* Ying Fan, and Kuang-Ta Chao

Department of Physics and State Key Laboratory of Nuclear Physics and Technology, Peking University, Beijing 100871, China

(Received 31 December 2009; published 26 April 2010)

In this paper, in the framework of nonrelativistic QCD we study the light hadron (LH) decays of the spin-triplet ($S = 1$) D-wave heavy quarkonia. The short-distance coefficients of all Fock states in the ${}^3D_J$ ($J = 1, 2, 3$) quarkonia including the D-wave color singlet, P-wave color octet, and S-wave color singlet and color octet are calculated perturbatively at α_s^3 order. The operator evolution equations of the four-fermion operators are also derived and are used to estimate the numerical values of the long-distance matrix elements. We find that for the $c\bar{c}$ system, the LH decay widths of $\psi(1^3D_J)$ predicted by nonrelativistic QCD is about $2 \sim 3$ times larger than the phenomenological potential model results, while for the $b\bar{b}$ system the two theoretical estimations of $\Gamma(\Upsilon(1^3D_J) \to \mathrm{LH})$ are in coincidence with each other. Our predictions for $\psi(1^3D_J)$ LH decay widths are $\Gamma(\psi(1^3D_J) \to \mathrm{LH}) = (435, 50, 172)$ keV for $J = 1, 2, 3$; and for $\Upsilon(1^3D_J)$, $\Gamma(\Upsilon(1^3D_J) \to \mathrm{LH}) = (6.91, 0.75, 2.75)$ keV for $J = 1, 2, 3$.

DOI: 10.1103/PhysRevD.81.074032 PACS numbers: 12.38.Bx, 12.39.Jh, 13.20.Gd

I. INTRODUCTION

The production, decay, and mass spectrum of heavy quarkonium have been interesting topics since the first charmonium state J/ψ was discovered in 1974. Because of their large mass scales and nonrelativistic nature, heavy quarkonia are good probes to study and understand quantum chromodynamics (QCD) from both perturbative and nonperturbative aspects. In fact, one of the earliest applications of QCD is to calculate the inclusive decay rates of heavy quarkonia. In early times, it was assumed that such a decay process can proceed through two steps. First, the heavy quarkonium transforms into a free $Q\bar{Q}$ pair, which is a long-distance nonperturbative effect. Then, the heavy-quark pair annihilates into light hadrons (LH) through gluons, which can be calculated perturbatively. In the nonrelativistic limit, the long-distance part is related to the $Q\bar{Q}$ Schrödinger wave functions or their derivatives at the origin. In this picture, the free $Q\bar{Q}$ are in color singlet and have the same quantum numbers J^{PC} as the bound state heavy quarkonium. This is referred to as the ''color-singlet model.'' Explicit calculations at next-to-leading order (NLO) in α_s for S-wave quarkonium decays support the color-singlet model factorization formula. But it breaks down in the calculations of P-wave [1,2] and D-wave [3,4] heavy quarkonium LH decays at α_s^3 order, where infrared divergences appear. Phenomenologically, these infrared divergences are regularized by the binding energy of $Q\bar{Q}$ bound states.

In Ref. [5], Bodwin, Braaten, and Lepage first introduced the color-octet matrix elements to absorb the infrared logarithms, then they developed nonrelativistic QCD (NRQCD) effective field theory [6], based on which the inclusive decay rate of heavy quarkonium can be given by a rigorous factorization formula, and calculated in a systematic way by double expansion of α_s, the coupling constant of QCD, and v, the typical velocity of heavy quarks in the heavy quarkonium. In their formula, heavy quarkonium is treated as a superposition state of $|Q\bar{Q}\rangle$, $|Q\bar{Q}g\rangle$, $|Q\bar{Q}gg\rangle$, and other higher order Fock states, rather than the $|Q\bar{Q}\rangle$ color-singlet state only. The contribution of each Fock state is organized in powers of v^2, and can be written as a product of the long-distance matrix element and the corresponding short-distance coefficient. Huang and Chao [7] first got the infrared finite LH decay width of the spin singlet P-wave state, h_c, with QCD radiative corrections in the framework of NRQCD. The decay widths of $\chi_{c_J} \to$ LH were calculated to α_s^3 order in Refs. [8,9]. Complete and detailed results of color-singlet and octet short-distance coefficients of S-wave and P-wave spin-triplet states were given in Ref. [10]. In Refs. [10,11], the authors also explained why the infrared divergences disappear in the NRQCD factorization approach.

NRQCD is now a widely accepted effective field theory for heavy quarkonium. In the framework of NRQCD, lots of theoretical work has been done to study S- and P-wave quarkonium decays, and some significant successes have been achieved (for a review see Ref. [12]). Recently, the order v^7 results of S- and P-wave heavy quarkonium inclusive hadronic decays were obtained by Brambilla *et al.* [13]. However, compared with S- and P-wave heavy quarkonium, little work has been done on D-wave states in NRQCD. In this paper, we will calculate the LH decay widths of spin-triplet D-wave states ${}^3D_J$ ($J = 1, 2, 3$). Here the subprocesses ${}^3S_1^{[1,8]} \to \mathrm{LH}$ and ${}^3P_J^{[8]} \to \mathrm{LH}$ at leading-order (LO) in v^2 are all included, in which the short-distance coefficients are calculated in a different way and in agreement with the results in Ref. [10]. As the main

*Present address: Departament d'Estructura i Constituents de la Matèria and Institut de Ciències del Cosmos, Universitat de Barcelona, Diagonal, 647, E-08028 Barcelona, Catalonia, Spain.

part of these D-wave quarkonium decays, the infrared safe short-distance coefficients of ${}^3D_J^{[1]} \to \mathrm{LH}$ are first obtained in this paper. We use the covariant projection method, which was first introduced in [14] and generalized in Refs. [10,15], to do the perturbative calculations. At LO in v^2, the long-distance matrix elements of color-singlet D-wave four-fermion operators are related to the wave function's second derivative at the origin. And the matrix elements of the S-wave and P-wave octet and of S-wave singlet four-fermion operators could be studied in lattice simulations, or determined by fitting experimental data, or roughly estimated through velocity scaling rules. To give numerical predictions, here we use operator evolution equations to estimate the values of the matrix elements. The rest of our paper is organized as follows: In Sec. II, we briefly introduce the NRQCD effective field theory and give the general formulas used in D dimension. In Sec. III, all the subprocesses will be calculated to α_s^3 order. And after matching the full QCD results with the NLO NRQCD ones, the infrared safe short-distance coefficients as well as the operator evolution equations are obtained in Sec. IV. In Sec. V, we will discuss the numerical results and their phenomenological applications to $c\bar{c}$ and $b\bar{b}$ systems.

II. GENERAL FORMULAS

The Lagrangian for NRQCD is [6]

$$\mathcal{L}_{\mathrm{NRQCD}} = \mathcal{L}_{\mathrm{light}} + \mathcal{L}_{\mathrm{heavy}} + \delta\mathcal{L}, \tag{1}$$

where $\mathcal{L}_{\mathrm{light}}$ includes gauge field and light quark parts, and $\mathcal{L}_{\mathrm{heavy}}$ is the nonrelativistic Lagrangian for the heavy quarks and antiquarks:

$$\mathcal{L}_{\mathrm{heavy}} = \psi^\dagger\left(iD_t + \frac{\mathbf{D}^2}{2m_Q}\right)\psi + \chi^\dagger\left(iD_t - \frac{\mathbf{D}^2}{2m_Q}\right)\chi, \tag{2}$$

where ψ and $\chi^\dagger$ are the Pauli spinor fields that annihilate heavy quark and antiquark, respectively, and D_t and $\mathbf{D}$ are the time and space components of the gauge-covariant derivative D^μ. $\delta\mathcal{L}$ describes the relativistic effects. The leading-order v^2 corrections are the bilinear terms:

$$\begin{aligned}\delta\mathcal{L}_{\mathrm{bilinear}} = {} & \frac{c_1}{8m_Q^3}[\psi^\dagger(\mathbf{D}^2)^2\psi - \chi^\dagger(\mathbf{D}^2)^2\chi] \\ & + \frac{c_2}{8m_Q^2}[\psi^\dagger(\mathbf{D}\cdot g\mathbf{E} - \mathbf{E}\cdot g\mathbf{D})\psi \\ & + \chi^\dagger(\mathbf{D}\cdot g\mathbf{E} - \mathbf{E}\cdot g\mathbf{D})\chi] \\ & + \frac{c_3}{8m_Q^2}[\psi^\dagger(i\mathbf{D}\times g\mathbf{E} - g\mathbf{E}\times i\mathbf{D})\cdot\boldsymbol{\sigma}\psi \\ & + \chi^\dagger(i\mathbf{D}\times g\mathbf{E} - g\mathbf{E}\times i\mathbf{D})\cdot\boldsymbol{\sigma}\chi] \\ & + \frac{c_4}{2m_Q}[\psi^\dagger(g\mathbf{B}\cdot\boldsymbol{\sigma})\psi - \chi^\dagger(g\mathbf{B}\cdot\boldsymbol{\sigma})\chi],\end{aligned} \tag{3}$$

where c_i could be obtained by using the Foldy-Wouthuysen-Tani transformation [16], diagonalizing the Dirac theory so as to decouple the heavy-quark and antiquark degrees of freedom. To reproduce the full QCD Lagrangian and to describe the annihilation of the heavy-quark pair, four-fermion local operator terms are also needed:

$$\delta\mathcal{L}_{\text{4-fermion}} = \sum_n \frac{f_n(\mu_\Lambda)}{m_Q^{d_n-4}}\mathcal{O}_n(\mu_\Lambda), \tag{4}$$

where $\mathcal{O}_n(\mu_\Lambda)$ is the local four-fermion operator with the general form $(\psi^\dagger\mathcal{K}_i\chi)(\chi^\dagger\mathcal{K}_i'\psi)$, and $f_n(\mu_\Lambda)$ is the Wilson coefficient. In effective theory both operators and coefficients are dependent on the factorization scale μ_Λ, but their combinations cancel the dependence. With the help of the optical theorem the inclusive decay rate of a heavy quarkonium state H could be expressed as

$$\begin{aligned}\Gamma(H \to \mathrm{LH}) &= 2\,\mathrm{Im}\langle H|\delta\mathcal{L}_{\text{4-fermion}}|H\rangle \\ &= \sum_n \frac{2\,\mathrm{Im} f_n(\mu_\Lambda)}{m_Q^{d_n-4}}\langle H|\mathcal{O}_n(\mu_\Lambda)|H\rangle.\end{aligned} \tag{5}$$

In principle, we need infinite terms to give theoretical predictions, but in practice only a finite number of these terms are needed to give an order of v^2 result, since the long-distance matrix elements can be ordered in powers of v^2 by applying the velocity scaling rules summarized in Ref. [6]. And the short-distance coefficients (Wilson coefficients), defined in the matching condition below, can be calculated perturbatively as a perturbation series in QCD coupling constant α_s

$$\begin{aligned}&\mathcal{A}(Q\bar{Q} \to Q\bar{Q})|_{\text{pert QCD}} \\ &\quad = \sum_n \frac{f_n(\mu_\Lambda)}{m^{d_n-4}}\langle Q\bar{Q}|\mathcal{O}_n^{Q\bar{Q}}(\mu_\Lambda)|Q\bar{Q}\rangle|_{\text{pert NRQCD}}.\end{aligned} \tag{6}$$

When quark and antiquark are in a particular angular momentum state J and color state 1 or 8, the imaginary part of the left-hand side of Eq. (6) can be calculated with the covariant projection method [10]:

$$\begin{aligned}&2\,\mathrm{Im}\mathcal{A}((Q\bar{Q})_{2S+1L_J}^{[1,8]} \to (Q\bar{Q})_{2S+1L_J}^{[1,8]})|_{\text{pert QCD}} \\ &\quad = \frac{\langle\mathcal{O}(^{2S+1}L_J)\rangle_{\mathrm{QCD}}}{K} \\ &\qquad \times \int\sum|\bar{\mathcal{M}}((Q\bar{Q})_{2S+1L_J}^{[1,8]} \to \mathrm{LH})|^2 d\Phi,\end{aligned} \tag{7}$$

where $\langle\mathcal{O}(^{2S+1}L_J)\rangle_{\mathrm{QCD}}$ equals to the corresponding NRQCD four-fermion operator expectation value at tree level, L is the orbital angular momentum, S is the total spin

of the heavy-quark pair, and K is the degree of freedom of the initial state. For spin-triplet states with $L=0$, $L=1$, and $L=2$, the relations between $\bar{\mathcal{M}}(Q\bar{Q})^{[1,8]}_{^3L_J}$ and the full QCD Feynman amplitude $\mathcal{M}$ are

$$\bar{\mathcal{M}}((Q\bar{Q})^{[1,8]}_{^3S_1}\to \mathrm{LH}) = \epsilon^{[S]}_{\rho}\mathrm{Tr}[\mathcal{C}^{[1,8]}\Pi^{\rho}\mathcal{M}]|_{q=0}, \tag{8a}$$

$$\bar{\mathcal{M}}((Q\bar{Q})^{[8]}_{^3P_{P_J}}\to \mathrm{LH}) = \epsilon^{[P_J]}_{\alpha\rho}\frac{d}{dq_\alpha}\mathrm{Tr}[\mathcal{C}^{[8]}\Pi^{\rho}\mathcal{M}]|_{q=0}, \tag{8b}$$

$$\bar{\mathcal{M}}((Q\bar{Q})^{[1]}_{^3D_{D_J}}\to \mathrm{LH}) = \frac{1}{2}\epsilon^{[D_J]}_{\alpha\beta\rho}\frac{d^2}{dq_\alpha dq_\beta} \times \mathrm{Tr}[\mathcal{C}^{[1]}\Pi^{\rho}\mathcal{M}]|_{q=0}, \tag{8c}$$

where ϵ^{s}_{ρ}, $\epsilon^{P_J}_{\alpha\rho}$, and $\epsilon^{D_J}_{\alpha\beta\rho}$ are the polarization tensors for $L=S,P,D$ states with total angular momentum 1, P_J, D_J, respectively. For spin-triplet states, the spin projector of the incoming heavy-quark pair accurate to all orders of v^2 is [15]

$$\Pi^{\rho} = -\frac{1}{2\sqrt{2}(E+m_Q)}\left(\frac{1}{2}\not{P}+\not{q}+m_Q\right) \times \frac{\not{P}+2E}{2E}\gamma^{\rho}\left(\frac{1}{2}\not{P}-\not{q}-m_Q\right), \tag{9}$$

where P^{μ} is the four momentum of the heavy meson and $P^2=4E^2$, and $2q^{\mu}$ is the relative momentum between the quark and antiquark. The color projectors are $\mathcal{C}^{[1]}=\frac{\delta_{i,j}}{\sqrt{N_c}}$ and $\mathcal{C}^{[8]}=\sqrt{2}(T_a)_{i,j}$.

In the Fock space, the $\psi(^3D_J)$ states are represented by

$$|^3D_J\rangle = \mathcal{O}(1)|Q\bar{Q}(^3D_J^{[1]})\rangle + \mathcal{O}(v)|Q\bar{Q}(^3P_J^{[8]})\rangle + \mathcal{O}(v^2)|Q\bar{Q}(^3S_J^{[1,8]})\rangle + \ldots. \tag{10}$$

Here, the probability of P-wave and S-wave states are suppressed by v^2 and v^4 relative to the D-wave state, respectively, but their operators scale as v^{-2} and v^{-4} relative to $\mathcal{O}_1(^3D_J)$. The relativistic effect and other Fock state contributions are suppressed at least by v^2. Thus at leading order in v^2 the NRQCD formula for ^3D_J decay into LH is

$$\begin{aligned}\Gamma(^3D_J\to \mathrm{LH}) &= 2\,\mathrm{Im}f(^3D_J^{[1]})\frac{\langle\psi(^3D_J)|\mathcal{O}_1(^3D_J)|\psi(^3D_J)\rangle}{m_Q^6} \\ &+ \sum_{J=0}^{2} 2\,\mathrm{Im}f(^3P_J^{[8]})\frac{\langle\psi(^3D_J)|\mathcal{O}_8(P_{^3J_P})|\psi(^3D_J)\rangle}{m_Q^4} \\ &+ 2\,\mathrm{Im}f(^3S_1^{[8]})\frac{\langle\psi(^3D_J)|\mathcal{O}_8(^3S_1)|\psi(^3D_J)\rangle}{m_Q^2} \\ &+ 2\,\mathrm{Im}f(^3S_1^{[1]})\frac{\langle\psi(^3D_J)|\mathcal{O}_1(^3S_1)|\psi(^3D_J)\rangle}{m_Q^2},\end{aligned} \tag{11}$$

where the four-fermion operators are defined[1] as

$$\mathcal{O}_1(^3S_1) = \frac{1}{2N_c}\psi^{\dagger}\boldsymbol{\sigma}\chi\cdot\chi^{\dagger}\boldsymbol{\sigma}\psi, \tag{12a}$$

$$\mathcal{O}_8(^3S_1) = \psi^{\dagger}\boldsymbol{\sigma}T^a\chi\cdot\chi^{\dagger}\boldsymbol{\sigma}T^a\psi, \tag{12b}$$

$$\mathcal{O}_8(^3P_0) = \frac{1}{3}\psi^{\dagger}\left(\frac{-i}{2}\overleftrightarrow{\boldsymbol{D}}\cdot\boldsymbol{\sigma}\right)T^a\chi\chi^{\dagger}\left(\frac{-i}{2}\overleftrightarrow{\boldsymbol{D}}\cdot\boldsymbol{\sigma}\right)T^a\psi, \tag{12c}$$

$$\mathcal{O}_8(^3P_1) = \frac{1}{2}\psi^{\dagger}\left(\frac{-i}{2}\overleftrightarrow{\boldsymbol{D}}\times\boldsymbol{\sigma}\right)T^a\chi\cdot\chi^{\dagger}\left(\frac{-i}{2}\overleftrightarrow{\boldsymbol{D}}\times\boldsymbol{\sigma}\right)T^a\psi, \tag{12d}$$

$$\mathcal{O}_8(^3P_2) = \frac{1}{2}\psi^{\dagger}\left(\frac{-i}{2}\overleftrightarrow{\boldsymbol{D}}^{(i}\boldsymbol{\sigma}^{j)}\right)T^a\chi\chi^{\dagger}\left(\frac{-i}{2}\overleftrightarrow{\boldsymbol{D}}^{(i}\boldsymbol{\sigma}^{j)}\right)T^a\psi, \tag{12e}$$

$$\mathcal{O}_1(^3D_1) = \frac{3}{10N_c}\psi^{\dagger}\boldsymbol{K}^i\chi\chi^{\dagger}\boldsymbol{K}^i\psi, \tag{12f}$$

$$\mathcal{O}_1(^3D_2) = \frac{1}{12N_c}\psi^{\dagger}\boldsymbol{K}^{ij}\chi\chi^{\dagger}\boldsymbol{K}^{ij}\psi, \tag{12g}$$

$$\mathcal{O}_1(^3D_3) = \frac{1}{18N_c}\psi^{\dagger}\boldsymbol{K}^{ijk}\chi\chi^{\dagger}\boldsymbol{K}^{ijk}\psi. \tag{12h}$$

The notations $\boldsymbol{K}$ are $\boldsymbol{K}^i=\boldsymbol{\sigma}^j\boldsymbol{S}^{ij}$, $\boldsymbol{K}^{ij}=\boldsymbol{\epsilon}^{ikl}\boldsymbol{\sigma}^l\boldsymbol{S}^{jk}+\boldsymbol{\epsilon}^{jkl}\boldsymbol{\sigma}^l\boldsymbol{S}^{ik}$, $\boldsymbol{K}^{ijk}=\boldsymbol{\sigma}^i\boldsymbol{S}^{jk}+\boldsymbol{\sigma}^j\boldsymbol{S}^{ki}+\boldsymbol{\sigma}^k\boldsymbol{S}^{ij}-\frac{2}{5}\boldsymbol{\sigma}^l(\delta^{jk}\boldsymbol{S}^{il}+\delta^{ki}\boldsymbol{S}^{jl}+\delta^{ij}\boldsymbol{S}^{kl})$, where $\boldsymbol{S}^{ij}=(\frac{-i}{2})^2(\overleftrightarrow{\boldsymbol{D}}^i\overleftrightarrow{\boldsymbol{D}}^j-\frac{1}{3}\overleftrightarrow{\boldsymbol{D}}^2\delta^{ij})$.

For some processes, we need to calculate the NLO QCD corrections. To handle the ultraviolet (UV) and infrared (IR) divergences in the dimensional regularization scheme, one should extend the projection method into $D=4-2\epsilon$ dimensions. The definitions of γ matrixes in D dimensions can be found in quantum field theory books. And the sums over polarization tensors $\epsilon^{[S]}_{\rho}$, $\epsilon^{[P_J]}_{\alpha\rho}$, and $\epsilon^{[D_J]}_{\alpha\beta\rho}$ in D dimension are

[1]The normalizations of the color-singlet four-fermion operators agree with those in Ref. [10]

$$\sum_{J_z} \epsilon^{(1)}_{\rho} \epsilon^{(1)*}_{\rho'} = \Pi_{\rho\rho'}, \tag{13a}$$

$$\sum_{J_z} \epsilon^{(0)}_{\alpha\rho} \epsilon^{(0)*}_{\alpha'\rho'} = \frac{1}{D-1} \Pi_{\alpha\rho} \Pi_{\alpha'\rho'}, \tag{13b}$$

$$\sum_{J_z} \epsilon^{(1)}_{\alpha\rho} \epsilon^{(1)*}_{\alpha'\rho'} = \frac{1}{2} (\Pi_{\alpha\alpha'} \Pi_{\rho\rho'} - \Pi_{\alpha\rho'} \Pi_{\alpha'\rho}), \tag{13c}$$

$$\sum_{J_z} \epsilon^{(2)}_{\alpha\rho} \epsilon^{(2)*}_{\alpha'\rho'} = \frac{1}{2} (\Pi_{\alpha\alpha'} \Pi_{\rho\rho'} + \Pi_{\alpha\rho'} \Pi_{\alpha'\rho}) - \frac{1}{D-1} \Pi_{\alpha\rho} \Pi_{\alpha'\rho'}, \tag{13d}$$

$$\begin{aligned} \sum_{J_z} \epsilon^{(1)}_{\alpha\beta\rho} \epsilon^{(1)*}_{\alpha'\beta'\rho'} = {} & \frac{D-1}{2(D-2)(D+1)} \Big(\Pi_{\alpha\rho} \Pi_{\alpha'\rho'} \Pi_{\beta\beta'} + \Pi_{\beta\rho} \Pi_{\beta'\rho'} \Pi_{\alpha\alpha'} + \Pi_{\alpha\rho} \Pi_{\beta'\rho'} \Pi_{\alpha'\beta} + \Pi_{\beta\rho} \Pi_{\alpha'\rho'} \Pi_{\alpha\beta'} \\ & - \frac{2}{D-1} (\Pi_{\alpha\rho} \Pi_{\alpha'\beta'} \Pi_{\beta\rho'} + \Pi_{\beta\rho} \Pi_{\alpha'\beta'} \Pi_{\alpha\rho'} + \Pi_{\alpha'\rho'} \Pi_{\alpha\beta} \Pi_{\beta'\rho} + \Pi_{\beta'\rho'} \Pi_{\alpha\beta} \Pi_{\alpha'\rho}) \\ & + \frac{4}{(D-1)^2} \Pi_{\alpha\beta} \Pi_{\alpha'\beta'} \Pi_{\rho\rho'} \Big), \end{aligned} \tag{13e}$$

$$\begin{aligned} \sum_{J_z} \epsilon^{(2)}_{\alpha\beta\rho} \epsilon^{(2)*}_{\alpha'\beta'\rho'} = {} & \frac{1}{6} (2\Pi_{\alpha\alpha'} \Pi_{\beta\beta'} \Pi_{\rho\rho'} + 2\Pi_{\alpha\beta'} \Pi_{\alpha'\beta} \Pi_{\rho\rho'} - \Pi_{\alpha\alpha'} \Pi_{\beta\rho'} \Pi_{\rho\beta'} - \Pi_{\alpha\beta'} \Pi_{\beta\rho'} \Pi_{\rho\alpha'} - \Pi_{\alpha\rho'} \Pi_{\beta\beta'} \Pi_{\rho\alpha'} \\ & - \Pi_{\alpha\rho'} \Pi_{\beta\alpha'} \Pi_{\rho\beta'}) + \frac{1}{6(D-2)} (-4\Pi_{\alpha\beta} \Pi_{\alpha'\beta'} \Pi_{\rho\rho'} + 2\Pi_{\alpha\rho'} \Pi_{\alpha'\beta'} \Pi_{\beta\rho} + 2\Pi_{\alpha\rho} \Pi_{\beta\rho'} \Pi_{\alpha'\beta'} \\ & + 2\Pi_{\alpha\beta} \Pi_{\alpha'\rho} \Pi_{\beta'\rho'} + 2\Pi_{\alpha\beta} \Pi_{\beta'\rho} \Pi_{\alpha'\rho'} - \Pi_{\alpha\beta'} \Pi_{\alpha'\rho'} \Pi_{\beta\rho} - \Pi_{\alpha\rho} \Pi_{\alpha'\beta} \Pi_{\beta'\rho'} - \Pi_{\alpha\alpha'} \Pi_{\beta\rho} \Pi_{\beta'\rho'} \\ & - \Pi_{\alpha\rho} \Pi_{\beta\beta'} \Pi_{\alpha'\rho'}), \end{aligned} \tag{13f}$$

$$\begin{aligned} \sum_{J_z} \epsilon^{(3)}_{\alpha\beta\rho} \epsilon^{(3)*}_{\alpha'\beta'\rho'} = {} & \frac{1}{6} (\Pi_{\alpha\alpha'} \Pi_{\beta\beta'} \Pi_{\rho\rho'} + \Pi_{\alpha\alpha'} \Pi_{\beta\rho'} \Pi_{\rho\beta'} + \Pi_{\alpha\beta'} \Pi_{\beta\alpha'} \Pi_{\rho\rho'} + \Pi_{\alpha\beta'} \Pi_{\beta\rho'} \Pi_{\rho\alpha'} + \Pi_{\alpha\rho'} \Pi_{\beta\beta'} \Pi_{\rho\alpha'} \\ & + \Pi_{\alpha\rho'} \Pi_{\beta\alpha'} \Pi_{\rho\beta'}) - \frac{1}{3(D+1)} (\Pi_{\alpha\beta} \Pi_{\rho\alpha'} \Pi_{\beta'\rho'} + \Pi_{\alpha\beta} \Pi_{\rho\beta'} \Pi_{\alpha'\rho'} + \Pi_{\alpha\beta} \Pi_{\rho\rho'} \Pi_{\alpha'\beta'} + \Pi_{\alpha\rho} \Pi_{\beta\alpha'} \Pi_{\beta'\rho'} \\ & + \Pi_{\alpha\rho} \Pi_{\beta\beta'} \Pi_{\alpha'\rho'} + \Pi_{\alpha\rho} \Pi_{\beta\rho'} \Pi_{\alpha'\beta'} + \Pi_{\beta\rho} \Pi_{\alpha\alpha'} \Pi_{\beta'\rho'} + \Pi_{\beta\rho} \Pi_{\alpha\beta'} \Pi_{\alpha'\rho'} + \Pi_{\beta\rho} \Pi_{\alpha\rho'} \Pi_{\alpha'\beta'}). \end{aligned} \tag{13g}$$

And the degrees of freedom are $D-1$ for the S-wave state; $1, \frac{(D-1)(D-2)}{2}, \frac{(D+1)(D-2)}{2}$ for $J=0,1,2$ P-wave states; and $D-1, \frac{(D-3)(D-1)(D+1)}{3}, \frac{(D-2)(D-1)(D+3)}{6}$ for $J=1,2,3$ D-wave states. The rather trivial extensions for $L=0$ and 1 cases were given in Ref. [10]. Here three principles are adopted to construct the nontrivial results for the D-wave case. First, the symmetry of the three indexes should be kept; second, the inner products between one tensor and the other two are zero; third, the completeness condition should be satisfied:

$$\begin{aligned} & \sum_{J_z} \epsilon^{(1)}_{\alpha\beta\rho} \epsilon^{(1)*}_{\alpha'\beta'\rho'} + \sum_{J_z} \epsilon^{(2)}_{\alpha\beta\rho} \epsilon^{(2)*}_{\alpha'\beta'\rho'} + \sum_{J_z} \epsilon^{(3)}_{\alpha\beta\rho} \epsilon^{(3)*}_{\alpha'\beta'\rho'} \\ & = \Big(\frac{1}{2} (\Pi_{\alpha\alpha'} \Pi_{\beta\beta'} + \Pi_{\alpha\beta'} \Pi_{\alpha'\beta}) - \frac{1}{D-1} \Pi_{\alpha\beta} \Pi_{\alpha'\beta'} \Big) \Pi_{\rho\rho'}. \end{aligned} \tag{14}$$

We calculate the degrees of freedom of each ${}^3D_J$ state with group theory and get Eq. (13e). Then we derive out Eq. (13g) with the help of the first two principles. In the end (13f) = (14) − (13e) − (13g).

To get the NLO NRQCD results, the operator mixing equation (15) between P-wave and D-wave operators in momentum space should also be extended into D dimension for consistency:

$$\begin{aligned} & \sum_{D_{J'}} C_{P_J, D_{J'}} \langle (Q\bar{Q})_{^3D_{J'}} | \mathcal{O}(^3D_{J'}) | (Q\bar{Q})_{^3D_{J'}} \rangle \\ & = \langle (Q\bar{Q})_{^3P_J} | \mathcal{O}(^3P_J) | (Q\bar{Q})_{^3P_J} \rangle \vec{q} \cdot \vec{q}', \end{aligned} \tag{15}$$

where $C_{P_J, D_{J'}}$ are the generalized Clebsch-Gordan coefficients:

$$C_{P_J, D_J} = \frac{|\epsilon^{\alpha\beta\rho(D_J)} \epsilon^{*(P_J)}_{\alpha\rho} \epsilon^{*(S=1)}_{\beta}|^2}{\epsilon^{(D_J)}_{\alpha'\beta'\rho'} \epsilon^{*\alpha'\beta'\rho'(D_J)}}, \tag{16}$$

where the repeated indexes mean being summed in D dimension.

After resolving the above problems, one can do calculations from both full QCD and NRQCD straightforwardly.

III. FULL QCD CALCULATION

In Sec. II, it has been explained that at leading order of v^2 the LH decays of ${}^3D_J$ contain the subprocesses of $Q\bar{Q}^{[1,8]}_{^3S_1}$, $Q\bar{Q}^{[8]}_{^3P_J}$ $(J=0,1,2)$, and $Q\bar{Q}^{[1]}_{^3D_J}$ $(J=0,1,2,3)$ annihilating into gluons or light quarks. When doing the

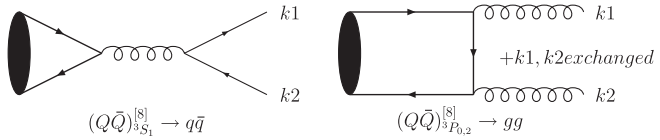

FIG. 1. Feynman diagrams for $(Q\bar{Q})^{[8]}_{^3S_1} \to q\bar{q}$, $(Q\bar{Q})^{[8]}_{^3P_{0,2}} \to gg$.

calculation with full QCD theory, for simplicity, only the explicit imaginary part of $\bar{\mathcal{A}}$ is given here

$$2\,\mathrm{Im}\bar{\mathcal{A}}((Q\bar{Q})^{[1,8]}_{^{2S+1}L_J} \to (Q\bar{Q})^{[1,8]}_{^{2S+1}L_J})|_{\text{pert QCD}} = \frac{1}{K}\int\sum|\bar{\mathcal{M}}((Q\bar{Q})^{[1,8]}_{^{2S+1}L_J} \to \mathrm{LH})|^2 d\Phi. \tag{17}$$

In the following subsections, the contributions at α_s^2 order, and the corresponding real and virtual corrections will be given in Secs. III A, III B, and III C respectively. As for the processes whose tree level diagrams are already at α_s^3 order, their results will also be given in Sec. III B.

A. LO results

There are three subprocesses $(Q\bar{Q})^{[8]}_{^3S_1} \to q\bar{q}$, $(Q\bar{Q})^{[8]}_{^3P_{0,2}} \to gg$ with nonvanishing imaginary parts at $\mathcal{O}(\alpha_s^2)$. The Feynman diagrams are shown in Fig. 1. And the results in D dimension are

$$(2\,\mathrm{Im}\bar{\mathcal{A}}(^3S_1^{[8]}))^{\mathrm{Born}} = \frac{1-\epsilon}{3-2\epsilon}\frac{8N_f\alpha_s^2\pi^2\mu^{4\epsilon}\Phi_{(2)}}{m_Q^2}, \tag{18a}$$

$$(2\,\mathrm{Im}\bar{\mathcal{A}}(^3P_0^{[8]}))^{\mathrm{Born}} = \frac{1-\epsilon}{3-2\epsilon}\frac{144B_F\alpha_s^2\pi^2\mu^{4\epsilon}\Phi_{(2)}}{m_Q^4}, \tag{18b}$$

$$(2\,\mathrm{Im}\bar{\mathcal{A}}(^3P_2^{[8]}))^{\mathrm{Born}} = \frac{4\epsilon^2-13\epsilon+6}{(3-2\epsilon)(5-2\epsilon)}\frac{32B_F\alpha_s^2\pi^2\mu^{4\epsilon}\Phi_{(2)}}{m_Q^4}, \tag{18c}$$

where $\Phi_{(2)} = \frac{1}{8\pi}\frac{\Gamma(1-\epsilon)}{\Gamma(2-2\epsilon)}(\frac{\pi}{m_Q^2})^\epsilon$ is the two-body phase space in D dimension.

B. Real corrections

Besides the real corrections (RC), other processes with three bodies in final states include $(Q\bar{Q})^{[1,8]}_{^3S_1} \to 3g$, $(Q\bar{Q})^{[8]}_{^3P_1} \to 3g$, $(Q\bar{Q})^{[8]}_{^3P_J} \to q\bar{q}g$, and $(Q\bar{Q})^{[1]}_{^3D_J} \to 3g$. And the typical Feynman diagrams for $q\bar{q}g$ and $3g$ are shown in Fig. 2 and 3, respectively.[2]

We calculate the Feynman amplitudes and do the phase space integrations both in D dimension, and check the results with eikonal approximation relations or Altarelli-Parisi splitting functions when one gluon is soft or two

[2]In the Feynman gauge the ghost diagrams are also needed, where a three-gluon or four-gluon vertex will appear.

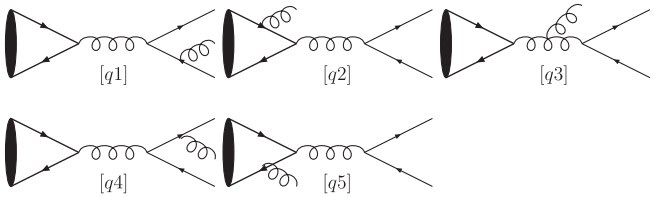

FIG. 2. Feynman diagrams for $(Q\bar{Q})^{[8]}_{^3L_J} \to q\bar{q}g$.

light partons (gluon or light quark) are collinear. Three variables $x_i = \frac{E_i}{m_Q}$ are introduced to describe the $(Q\bar{Q})_{^3L_J^{[1,8]}} \to k_1 + k_2 + k_3$ process. For energy conservation $x_1 + x_2 + x_3 = 2$. The three-body phase space in D dimension becomes

$$d\Phi_{(3)} = \Phi_{(2)}\frac{4m_Q^2}{(4\pi)^2\Gamma(1-\epsilon)}\left(\frac{\pi}{m_Q^2}\right)^\epsilon[(1-x_1)(1-x_2) \times (1-x_3)]^{-\epsilon}\delta(2-x_1-x_2-x_3)dx_1dx_2dx_3. \tag{19}$$

In the phase space, the $x_i = 0$ region is the soft region of particle with momentum k_i, and the $x_i = 1$ region is the collinear region of the other two particles. And the inner products of those four momenta are $P \cdot k_i = 2m_Q^2 x_i$, $k_i \cdot k_j = 2m_Q^2(x_i + x_j - 1)$.

When $L = S$ and P, the real corrections contributing to $2\,\mathrm{Im}\bar{\mathcal{A}}(^3L_J^{[1,8]})^{\mathrm{RC}}$ are

$$2\,\mathrm{Im}\bar{\mathcal{A}}(^3L_J^{[1,8]})^{\mathrm{RC}} = \frac{1}{3!(K_{c1,c8})(K_J)} \times \int\sum|\bar{\mathcal{M}}((Q\bar{Q})^{[1,8]}_{^3L_J} \to ggg)|^2 d\Phi_{(3)} + \frac{1}{(K_{c1,c8})(K_J)} \times \int\sum|\bar{\mathcal{M}}((Q\bar{Q})^{[1,8]}_{^3L_J} \to q\bar{q}g)|^2 d\Phi_{(3)}, \tag{20}$$

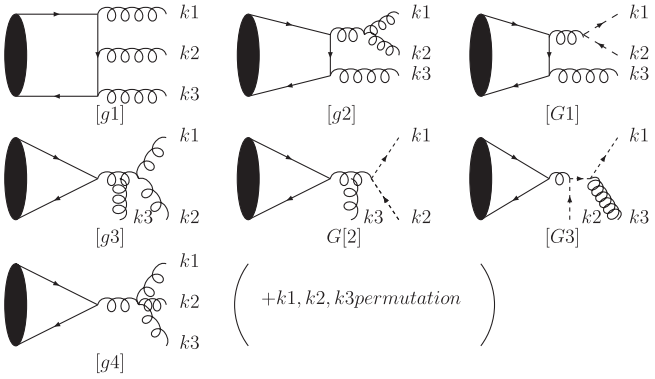

FIG. 3. Feynman diagrams for $(Q\bar{Q})_{^3L_J^{[1,8]}} \to 3g$. Diagrams with different positions of k_i are neglected. In Feynman gauge the ghost diagrams should also be contained.

where $K_{c1}=1$, $K_{c8}=N_c^2-1$, and K_J is the polarization number of angular momentum J state. In the D-wave case, because of parity conservation, only the $3g$ process is left.

1. $(Q\bar{Q})_{^3L_J^{[1,8]}} \to ggg$

There are 18 diagrams in the $Q\bar{Q} \to ggg$ process. Because of J^{PC} conservation, only class [g1] is needed in $^3S_1^{[1]} \to ggg$ and $^3D_J^{[1]} \to ggg$ processes. In the $^3P_J^{[8]} \to ggg$ processes, the diagrams are those in class [g1], class [g2] and the corresponding ghost ones in class [G1]. And all the diagrams should be calculated in the $^3S_1^{[8]} \to ggg$ case. We now proceed to show how to get the physical results at a differential cross section level when ghost diagrams are contained. In the Feynman gauge, when the three or four gluon vertex appears, the nonphysical (NP) degrees of freedom are removed by ghost diagrams. Label the square of the amplitudes of the gluon diagrams in the Feynman gauge with the subscript NP, and express the ghost result as

$$|\bar{M}_G|^2_{k_i,k_j} = \sum |\bar{\mathcal{M}}((Q\bar{Q})^{[1,8]}_{^3L_J} \to g G_{k_i} \bar{G}_{k_j})|^2, \tag{21}$$

where G_{k_i} and $\bar{G}_{k_j}$ are for ghost and antighost with momentum k_i and k_j, respectively. To cancel the NP part of each gluon, all possibilities of indexes i, j should be summed over. Then proper physical results at the differential level are

$$\sum |\bar{\mathcal{M}}((Q\bar{Q})^{[1,8]}_{^3L_J} \to ggg)|^2 = \sum |\bar{\mathcal{M}}_{NP}((Q\bar{Q})^{[1,8]}_{^3L_J} \to ggg)|^2 - \sum_{i,j} |\bar{M}_G|^2_{k_i,k_j}. \tag{22}$$

Here we omit the details and only give the real corrections below

$$\frac{1}{3!(3-2\epsilon)} \int \sum |\bar{\mathcal{M}}((Q\bar{Q})^{[1]}_{^3S_1} \to ggg)|^2 d\Phi_{(3)} = \frac{40\alpha_s^3(\pi^2-9)}{81 m_Q^2}, \tag{23a}$$

$$\frac{1}{3!(N_C^2-1)(3-2\epsilon)} \int \sum |\bar{\mathcal{M}}((Q\bar{Q})^{[8]}_{^3S_1} \to ggg)|^2 d\Phi_{(3)} = \frac{5(67\pi^2-657)\alpha_s^3}{108 m_Q^2}, \tag{23b}$$

$$\frac{1}{3!(N_C^2-1)} \int \sum |\bar{\mathcal{M}}((Q\bar{Q})^{[8]}_{^3P_0} \to ggg)|^2 d\Phi_{(3)} = \frac{C_A \alpha_s F_\epsilon}{\pi}\left(\frac{1}{\epsilon^2}+\frac{7}{3\epsilon}+\frac{875-60\pi^2}{162}\right)(2\,\mathrm{Im}\bar{\mathcal{A}}(^3P_0^{[8]}))^{\mathrm{Born}}, \tag{23c}$$

$$\frac{2}{3!(N_C^2-1)(3-2\epsilon)(2-2\epsilon)} \int \sum |\bar{\mathcal{M}}((Q\bar{Q})^{[8]}_{^3P_1} \to ggg)|^2 d\Phi_{(3)} = \frac{C_A B_F(-138\pi^2+1369)\alpha_s^3}{54 m_Q^4}, \tag{23d}$$

$$\frac{2}{3!(N_C^2-1)(5-2\epsilon)(2-2\epsilon)} \int \sum |\bar{\mathcal{M}}((Q\bar{Q})^{[8]}_{^3P_2} \to ggg)|^2 d\Phi_{(3)} = \frac{C_A \alpha_s F_\epsilon}{\pi}\left(\frac{1}{\epsilon^2}+\frac{7}{3\epsilon}+\frac{4679-438\pi^2}{432}\right) \times (2\,\mathrm{Im}\bar{\mathcal{A}}(^3P_2^{[8]}))^{\mathrm{Born}}, \tag{23e}$$

$$\frac{1}{3!(3-2\epsilon)} \int \sum |\bar{\mathcal{M}}((Q\bar{Q})^{[1]}_{^3D_1} \to ggg)|^2 d\Phi_{(3)} = \frac{32}{3m_Q^6} B_F \Phi_2 F_\epsilon \pi \alpha_s^3 \mu^{4\epsilon}\left(-\frac{608}{135\epsilon}+\frac{-7744+1605\pi^2}{16\,200}\right), \tag{23f}$$

$$\frac{3}{3!(5-2\epsilon)(3-2\epsilon)(1-2\epsilon)} \int \sum |\bar{\mathcal{M}}((Q\bar{Q})^{[1]}_{^3D_2} \to ggg)|^2 d\Phi_{(3)} = \frac{32}{3m_Q^6} B_F \Phi_2 F_\epsilon \pi \alpha_s^3 \mu^{4\epsilon}\left(-\frac{8}{15\epsilon}+\frac{-23\,024+2125\pi^2}{1800}\right), \tag{23g}$$

$$\frac{6}{3!(7-2\epsilon)(3-2\epsilon)(2-2\epsilon)} \int \sum |\bar{\mathcal{M}}((Q\bar{Q})^{[1]}_{^3D_3} \to ggg)|^2 d\Phi_{(3)} = \frac{32}{3m_Q^6} B_F \Phi_2 F_\epsilon \pi \alpha_s^3 \mu^{4\epsilon}\left(-\frac{32}{15\epsilon}+\frac{-28\,656+2645\pi^2}{6300}\right), \tag{23h}$$

where the "=" are correct at $\mathcal{O}(1)$, $F_\epsilon = (\frac{\pi\mu^2}{m_Q^2})^\epsilon \Gamma(1+\epsilon)$, $C_A=3$, and $B_F=5/12$ are color factors. The expressions of $\sum |\bar{\mathcal{M}}((Q\bar{Q})^{[1]}_{^3D_J} \to ggg)|^2$ are too complicated to be given here.

2. $(Q\bar{Q})_{^3L_J^{[1,8]}} \to q\bar{q}g$

At $\mathcal{O}(\alpha_s^3)$ there are four subprocesses: $(Q\bar{Q})_{^3S_1^{[8]}} \to q\bar{q}g$, which include all the Feynman diagrams in Fig. 2, and $(Q\bar{Q})_{^3P_J^{[8]}} \to q\bar{q}g$, in which there are only two diagrams $q[2]$ and $q[5]$. As in the $3g$ processes both the Feynman amplitudes

and the phase space integrals are calculated in D dimension directly and the results are

$$\frac{1}{(N_c^2-1)(3-2\epsilon)}\int\sum|\bar{\mathcal{M}}((Q\bar{Q})^{[8]}_{^3S_1}\to q\bar{q}g)|^2d\Phi_{(3)}=\frac{\alpha_s F_\epsilon}{\pi}\Big(C_F\Big(\frac{1}{\epsilon^2}+\frac{3}{2\epsilon}+\frac{57-8\pi^2}{12}\Big)+C_A\Big(\frac{1}{2\epsilon}+\frac{11}{6}\Big)\Big)(2\,\mathrm{Im}\bar{\mathcal{A}}(^3S_1^{[8]}))^{\mathrm{Born}}, \tag{24a}$$

$$\frac{1}{(N_c^2-1)}\int\sum|\bar{\mathcal{M}}((Q\bar{Q})^{[8]}_{^3P_0}\to q\bar{q}g)|^2d\Phi_{(3)}=\Big(N_f\frac{\alpha_s F_\epsilon}{\pi}\Big(-\frac{1}{3\epsilon}\Big)\Big)(2\,\mathrm{Im}\bar{\mathcal{A}}(^3P_0^{[8]}))^{\mathrm{Born}}-\frac{4}{9m_Q^2}B_F\alpha_s\Big(3(2\,\mathrm{Im}\bar{\mathcal{A}}(^3S_1^{[8]}))^{\mathrm{Born}}\frac{F_\epsilon}{\pi\epsilon}+\frac{29N_f}{3m_Q^2}\alpha_s^2\Big), \tag{24b}$$

$$\frac{1}{(N_c^2-1)}\int\sum|\bar{\mathcal{M}}((Q\bar{Q})^{[8]}_{^3P_1}\to q\bar{q}g)|^2d\Phi_{(3)}=\Big(N_f\frac{\alpha_s F_\epsilon}{\pi}\Big(-\frac{1}{3\epsilon}\Big)\Big)(2\,\mathrm{Im}\bar{\mathcal{A}}(^3P_1^{[8]}))^{\mathrm{Born}}-\frac{4}{9m_Q^2}B_F\alpha_s\Big(3(2\,\mathrm{Im}\bar{\mathcal{A}}(^3S_1^{[8]}))^{\mathrm{Born}}\frac{F_\epsilon}{\pi\epsilon}+\frac{8N_f}{3m_Q^2}\alpha_s^2\Big), \tag{24c}$$

$$\frac{1}{(N_c^2-1)}\int\sum|\bar{\mathcal{M}}((Q\bar{Q})^{[8]}_{^3P_2}\to q\bar{q}g)|^2d\Phi_{(3)}=\Big(N_f\frac{\alpha_s F_\epsilon}{\pi}\Big(-\frac{1}{3\epsilon}\Big)\Big)(2\,\mathrm{Im}\bar{\mathcal{A}}(^3P_2^{[8]}))^{\mathrm{Born}}-\frac{4}{9m_Q^2}B_F\alpha_s\Big(3(2\,\mathrm{Im}\bar{\mathcal{A}}(^3S_1^{[8]}))^{\mathrm{Born}}\frac{F_\epsilon}{\pi\epsilon}+\frac{58N_f}{15m_Q^2}\alpha_s^2\Big). \tag{24d}$$

C. Virtual corrections

The virtual corrections are performed with a renormalized Lagrangian, in which the renormalization constants of the QCD gauge coupling constant $g_s=\sqrt{4\pi\alpha_s}$, heavy-quark m_Q, heavy-quark field ψ_Q, light quark field ψ_q, and gluon field $\mathcal{A}_\mu$ are defined as

$$g_s^0=Z_g g_s,\qquad m_Q^0=Z_{m_Q}m_Q,\qquad \psi_Q^0=\sqrt{Z_{2Q}}\psi,\qquad \psi_q^0=\sqrt{Z_{2q}}\psi,\qquad \mathbf{A}_\mu^0=\sqrt{Z_3}\mathcal{A}_\mu, \tag{25}$$

where the superscript 0 labels bare quantities, and $Z_i=1+\delta_i$. Here a mixing renormalization scheme [17] is adopted. The quark mass m_Q, heavy-quark field ψ_Q, light quark field ψ_q, and gluon field $\mathbf{A}_\mu$ are defined in the on-shell condition, while g_s is in the minimal-subtraction($\overline{MS}$) scheme. Then in this mixing scheme, these renormalization constants are

$$\delta Z_{2Q}^{OS}=-\frac{C_F\alpha_s F_\epsilon}{4\pi}\Big(\frac{1}{\epsilon_{UV}}+\frac{2}{\epsilon_{IR}}+3\ln(4)+4+\mathcal{O}(\epsilon)\Big), \tag{26a}$$

$$\delta Z_{2q}^{OS}=-\frac{C_F\alpha_s F_\epsilon}{4\pi}\Big(\frac{1}{\epsilon_{UV}}-\frac{1}{\epsilon_{IR}}+\mathcal{O}(\epsilon)\Big), \tag{26b}$$

$$\delta Z_3^{OS}=\frac{\alpha_s F_\epsilon}{4\pi}(\beta_0-C_A)\Big(\frac{2}{\epsilon_{UV}}-\frac{2}{\epsilon_{IR}}+\mathcal{O}(\epsilon)\Big), \tag{26c}$$

$$\delta Z_{m_Q}^{OS}=-\frac{3C_F\alpha_s F_\epsilon}{4\pi}\Big(\frac{1}{\epsilon_{UV}}+\ln(4)+\frac{4}{3}+\mathcal{O}(\epsilon)\Big), \tag{26d}$$

$$\delta Z_g^{\overline{MS}}=-\frac{\beta_0\alpha_s F_\epsilon}{4\pi}\Big(\frac{1}{\epsilon_{UV}}-\ln\Big(\frac{\mu^2}{4m_Q^2}\Big)+\mathcal{O}(\epsilon)\Big), \tag{26e}$$

where $\beta_0=\frac{11C_A}{6}-\frac{N_f}{3}$, and N_f is the number of light flavor quarks. The representative virtual correction Feynman diagrams for the Born processes in Sec. III A are shown in Figs. 4 and 5, without external leg correction diagrams in this scheme. The UV divergences in self-energy and triangle diagrams will be canceled by the counterterm diagrams correspondingly. To regularize the Coulomb $\frac{1}{v}$ poles in the virtual processes, the loop integrals are done first before setting the relative momentum $q=0$. Also in $(Q\bar{Q})^{[8]}_{^3P_{0,2}}\to gg$ processes, we integrate the loop momentum first then compute the first derivative of the Feynman amplitudes with respect to q^α. When $q\neq 0$, the momenta of Q and $\bar{Q}$ are $P_Q=\frac{P}{2}+q$, $P_{\bar{Q}}=\frac{P}{2}-q$, where P is the meson total momentum, and the momenta of the two massless final state particles are labeled with k_1 and k_2. Then the scalar functions of the loop integrals can be expressed in the Mandelstam variables:

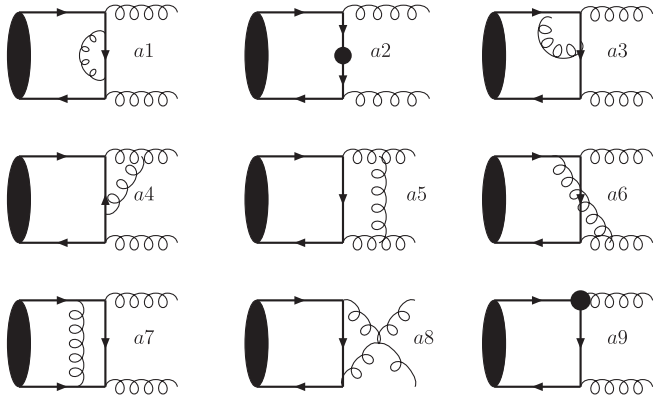

FIG. 4. One-loop Feynman diagram for $(Q\bar{Q})_{^3P^{[8]}_{0,2}}\to gg$.

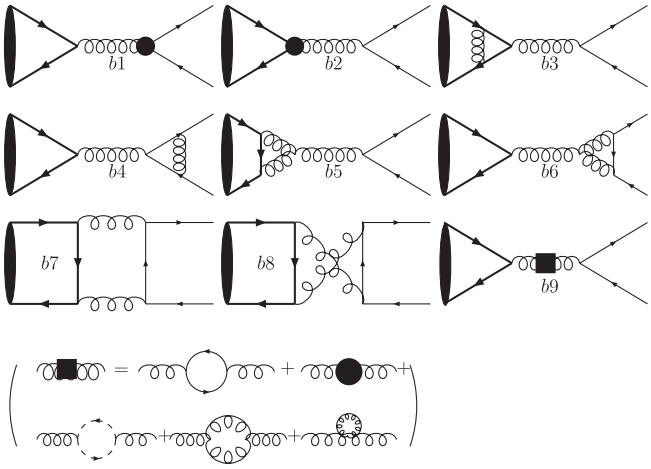

FIG. 5. One-loop Feynman diagram for $(Q\bar{Q})_{^3S_1^{[8]}} \to q\bar{q}$.

$$s = (P_Q + P_{\bar{Q}})^2, \qquad t = (P_Q - k_1)^2, \qquad u = (P_Q - k_2)^2, \tag{27}$$

where $s = 4m_Q^2/(1 - v^2)$. We do the calculations diagram by diagram and summarize the results in the following form:

$$2\,\mathrm{Im}\bar{\mathcal{A}}(^3L_J^{[1,8]})^{VC} = 2\,\mathrm{Im}\bar{\mathcal{A}}(^3L_J^{[1,8]})^{\mathrm{Born}}\frac{\alpha_s F_\epsilon}{\pi}\sum_k D_k, \tag{28}$$

where D_k for each process are listed in Table I, II, and III. The contributions of the counter-term diagrams are put together with the corresponding self-energy and vertex diagrams to show explicit cancelation of the UV divergences. The IR divergences left will be canceled by the RC.

D. Summation of real and virtual corrections

Collecting the RC with virtual correction, we obtain the full QCD results at $\mathcal{O}(\alpha_s^3)$:

TABLE I. Virtual corrections to $(Q\bar{Q})_{^3S_1^{[8]}} \to q\bar{q}$.

Diag.	D_k
$b1 + b4 + b6$	$\frac{C_A-2C_F}{2\epsilon_{IR}^2} + \frac{C_A-3C_F-\beta_0}{2\epsilon_{IR}} + \frac{C_A(9-2\pi^2)+4C_F(-6+\pi^2)}{6} + \frac{\beta_0}{2}\ln(\frac{\mu^2}{4m_Q^2})$
$b2 + b3 + b5$	$\frac{(2C_F-C_A)\pi^2}{4v} - \frac{\beta_0}{2\epsilon_{IR}} + \frac{C_A(7+2\ln(2))-12C_F}{3} + \frac{\beta_0}{2}\ln(\frac{\mu^2}{4m_Q^2})$
$b7$	$(2C_F - \frac{C_A}{2})(\frac{\pi^2}{6} - \frac{1}{\epsilon_{IR}^2})$
$b8$	$(2C_F - C_A)(\frac{1}{\epsilon_{IR}^2} - \frac{\pi^2}{6})$
$b9$	$(\frac{5}{6}C_A - \frac{1}{3}N_f)\frac{1}{\epsilon_{IR}} + \frac{31}{18}C_A - \frac{5}{9}N_f$

TABLE II. Virtual corrections to $(Q\bar{Q})_{^3P_0^{[8]}} \to gg$.

Diag.	D_k
$a1 + a2$	$\frac{C_F}{\epsilon_{IR}} + \frac{C_F(5+32\ln(2))}{9}$
$a3 + a4 + a9$	$\frac{-C_A}{3\epsilon_{IR}^2} + \frac{-9\beta_0-C_A-18C_F}{9\epsilon_{IR}} + \frac{C_F(-44-128\ln(2)+3\pi^2)}{18} + \frac{C_A(38+8\ln(2)-\pi^2)}{36} + \beta_0\ln(\frac{\mu^2}{4m_Q^2})$
$a5$	$\frac{C_A}{2}(\frac{-4}{3\epsilon_{IR}^2} + \frac{2}{9\epsilon_{IR}} - \frac{14}{27} + \frac{13}{18}\pi^2 + \frac{14}{27}\ln(2))$
$a6$	0
$a7$	$(C_F - \frac{C_A}{2})(\frac{1}{\epsilon_{IR}} + \frac{\pi^2}{2v} - \frac{4}{9} + \frac{1}{12}\pi^2 + \frac{32}{9}\ln(2))$
$a8$	$C_A(\frac{-19}{27} + \frac{70}{27}\ln(2))$

TABLE III. Virtual corrections to $(Q\bar{Q})_{^3P_2^{[8]}} \to gg$.

Diag.	D_k
$a1 + a2$	$C_F(\frac{1}{\epsilon_{IR}} + \frac{11}{6} + \frac{29}{6}\ln(2))$
$a3 + a4 + a9$	$\frac{-3C_A}{16\epsilon_{IR}^2} + \frac{-32\beta_0+15C_A-64C_F}{32\epsilon_{IR}} - \frac{C_F(100+172\ln(2)+3\pi^2)}{24} + \frac{C_A(75+112\ln(2)+18\pi^2)}{192} + \beta_0\ln(\frac{\mu^2}{4m_Q^2})$
$a5$	$\frac{C_A}{2}(-\frac{13}{8\epsilon_{IR}^2} - \frac{15}{16\epsilon_{IR}} - \frac{17}{288} + \frac{37}{48}\pi^2 + \frac{89}{18}\ln(2))$
$a6$	0
$a7$	$(C_F - \frac{C_A}{2})(\frac{1}{\epsilon_{IR}} + \frac{1}{2v}\pi^2 - \frac{5}{3} + \frac{1}{8}\pi^2 + \frac{7}{3}\ln(2))$
$a8$	$-C_A(\frac{5}{9} + \frac{10}{9}\ln(2))$

$$(2\,\mathrm{Im}\bar{\mathcal{A}}(^3S_1^{[1]}))|_{\mathrm{pert\ QCD}} = \frac{40\alpha_s^3(\pi^2-9)}{81m_Q^2}, \tag{29a}$$

$$(2\,\mathrm{Im}\bar{\mathcal{A}}(^3S_1^{[8]}))|_{\mathrm{pert\ QCD}} = \frac{\alpha_s^2}{108m_Q^2}\Big(5\alpha_s(-657+67\pi^2)+N_f\Big(36\pi+\alpha_s\Big(36(2C_F-C_A)\frac{\pi^2}{4v}+642-20N_f - 27\pi^2+72\ln(2)+36\beta_0\ln\frac{\mu^2}{4m_Q^2}\Big)\Big)\Big), \tag{29b}$$

$$(2\,\mathrm{Im}\bar{\mathcal{A}}(^3P_0^{[8]}))|_{\mathrm{pert\ QCD}} = \frac{5\alpha_s^2}{432m_Q^4}\Big(216\pi+\alpha_s\Big(54(2C_F-C_A)\frac{\pi^2}{v}+3032+21\pi^2+840\ln(2) + 216\beta_0\ln\Big(\frac{\mu^2}{4m_Q^2}\Big)\Big)\Big)-\frac{4}{9m_Q^2}B_F\alpha_s\Big(3(2\,\mathrm{Im}\mathcal{A}(^3S_1^{[8]}))^{\mathrm{Born}}\frac{F_\epsilon}{\pi\epsilon}+\frac{29N_f}{3m_Q^2}\alpha_s^2\Big), \tag{29c}$$

$$(2\,\mathrm{Im}\bar{\mathcal{A}}(^3P_1^{[8]}))|_{\mathrm{pert\ QCD}} = \frac{5\alpha_s^2(1369-138\pi^2)}{216m_Q^4}-\frac{4}{9m_Q^2}B_F\alpha_s\Big(3(2\,\mathrm{Im}\mathcal{A}(^3S_1^{[8]}))^{\mathrm{Born}}\frac{F_\epsilon}{\pi\epsilon}+\frac{8N_f}{3m_Q^2}\alpha_s^2\Big), \tag{29d}$$

$$(2\,\mathrm{Im}\bar{\mathcal{A}}(^3P_2^{[8]}))|_{\mathrm{pert\ QCD}} = \frac{\alpha_s^2}{216m_Q^4}\Big(144\pi+\alpha_s\Big(36(2C_F-C_A)\frac{\pi^2}{v}+4187-258\pi^2+336\ln(2) + 144\beta_0\ln\Big(\frac{\mu^2}{4m_Q^2}\Big)\Big)\Big)-\frac{4}{9m_Q^2}B_F\alpha_s\Big(3(2\,\mathrm{Im}\mathcal{A}(^3S_1^{[8]}))^{\mathrm{Born}}\frac{F_\epsilon}{\pi\epsilon}+\frac{58N_f}{15m_Q^2}\alpha_s^2\Big), \tag{29e}$$

$$(2\,\mathrm{Im}\bar{\mathcal{A}}(^3D_1^{[1]}))|_{\mathrm{pert\ QCD}} = \frac{32}{3m_Q^6}B_F\Phi_2F_\epsilon\pi\alpha_s^3\mu^{4\epsilon}\Big(-\frac{608}{135\epsilon}+\frac{-7744+1605\pi^2}{16\,200}\Big), \tag{29f}$$

$$(2\,\mathrm{Im}\bar{\mathcal{A}}(^3D_2^{[1]}))|_{\mathrm{pert\ QCD}} = \frac{32}{3m_Q^6}B_F\Phi_2F_\epsilon\pi\alpha_s^3\mu^{4\epsilon}\Big(-\frac{8}{15\epsilon}+\frac{-23\,024+2125\pi^2}{1800}\Big), \tag{29g}$$

$$(2\,\mathrm{Im}\bar{\mathcal{A}}(^3D_3^{[1]}))|_{\mathrm{pert\ QCD}} = \frac{32}{3m_Q^6}B_F\Phi_2F_\epsilon\pi\alpha_s^3\mu^{4\epsilon}\Big(-\frac{32}{15\epsilon}+\frac{-28\,656+2645\pi^2}{6300}\Big). \tag{29h}$$

There are still infrared divergences and Coulomb singularities in some of the expressions above. As explained in Ref. [6], the infrared divergence comes from the soft gluon emission of heavy quarks, and the Coulomb singularity reflects the behavior of heavy quarks in the potential region. In next section, both of them will be repeated precisely when doing the NLO corrections for NRQCD matrix elements in the corresponding regions.

As mentioned above, the S- and P-wave subprocesses have been studied by Petrelli *et al.* [10]. In their paper, the soft and collinear singularities are separated with the help of eikonal approximation and Altarelli-Pasrisi splitting functions, then they calculate the finite part in 4 dimension. In this paper, we recalculate them in D dimension directly as a cross check, and get the same results. The D-wave subprocesses have also been considered in Refs. [3,4] but they did the calculations in 4 dimension, and regularized the infrared divergence with the binding energy.

IV. NRQCD RESULT AND OPERATOR EVOLUTION EQUATIONS

There are three typical energy scales in the heavy quarkonium system, related to the small parameter v. They are m_Q (the heavy-quark mass), $m_Q v$ (the typical momentum of heavy quarks in heavy quarkonium), and $m_Q v^2$ (the binding energy). Then, there are three dynamical regimes in the NRQCD effective theory, in which either the heavy-quark or the gluon is on mass shell, and they are

$$\begin{aligned}
&\text{soft regime: } A_s^\mu\text{: } k_0 \sim |\vec{k}| \sim m_Q v,\\
&\qquad\qquad \Psi_s\text{: } T \sim |\vec{p}| \sim m_Q v,\\
&\text{potential regime: } A_p^\mu\text{: } k_0 \sim m_Q v^2, \qquad |\vec{k}| \sim m_Q v,\\
&\qquad\qquad \Psi_p\text{: } T \sim m_Q v^2, \qquad |\vec{p}| \sim m_Q v,\\
&\text{ultrasoft regime: } A_u^\mu\text{: } k_0 \sim |\vec{k}| \sim m_Q v^2,
\end{aligned} \tag{30}$$

where k_ν and p_ν are the momenta of the gluon field and heavy-quark field, respectively, and $T = p_0 - m_Q = \frac{\vec{p}^2}{2m_Q} + \mathcal{O}(v^4)$. Because there are more than one regimes in the nonrelativistic system, matching the production and annihilation of external heavy-quark and antiquark pairs at certain order in v can not be manifest, though the power counting rule, velocity scaling rule, of operators in NRQCD is simple. This problem has been addressed in several papers [18–25], and the matching prescriptions based on dimensional regularization in NRQCD were also clarified. Furthermore, the potential NRQCD (pNRQCD) effective theory was proposed by introducing the potential to manage the nonperturbative effect in

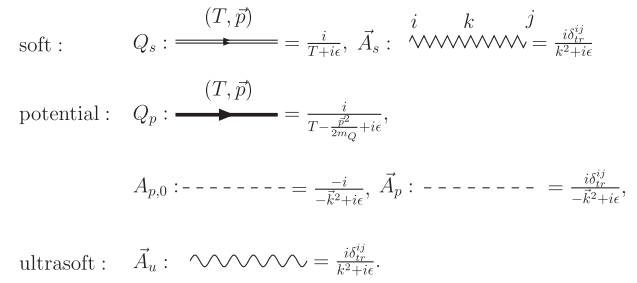

FIG. 6. NRQCD Feynman rules for heavy-quark and gloun propagators in different regimes.

Ref. [26]. The NRQCD Feynman rules for propagators in the Coulomb gauge [25], are shown in Fig. 6, where $\delta_{tr}^{ij} = \delta_{ij} - \frac{k^i k^j}{|\mathbf{k}|^2}$. At leading order in v^2, the interaction term of the NRQCD Lagrangian, where the antiheavy terms are neglected, is $ig_s\psi^\dagger(A_0 + \frac{(\mathbf{A}\cdot\boldsymbol{\nabla}+\boldsymbol{\nabla}\cdot\mathbf{A})}{2m_Q})\psi$. And it turns to be $ig_s\psi^\dagger(A_0 + \frac{\mathbf{A}\cdot\boldsymbol{\nabla}}{m_Q})\psi$, for $\boldsymbol{\nabla}\cdot\mathbf{A} = 0$ in the Coulomb gauge. The Feynman rules for vertex can be read directly and are listed in Fig. 7.[3] The Feynman rules for anti-heavy quark can be gotten by charge-conjugation symmetry.

Since the short-distance coefficients are obtained by matching full QCD results with NRQCD results, we only need to calculate the real parts of the matrix elements. Figure 8 gives the LO Feynman diagram. At NLO in α_s, when the inner gluon line joints two incoming or outgoing quark lines, a nonvanishing real part only appears in the potential region. When the inner gluon line connects with one incoming quark line and one outgoing quark line, the power counting rules [25] tell us that the soft region will provide the leading order contribution in v. The external self-energy diagrams are dropped to be in accordance with the renormalization scheme in full QCD calculation. Then we only need to calculate, two class, six NLO Feynman diagrams shown in Fig. 9.

For convenience, we present the detailed NLO corrections of the P-wave octet matrix elements, $\langle\mathcal{O}(^3P_J^{[8]})\rangle$, which are more representative than the S-wave ones. The LO result $\langle\mathcal{O}(^3P_J^{[8]})\rangle_{\text{Born}}$ is trivial. Using the Feynman rules for propagators in the soft regime and vertices, the loop integral of diagram (a) reads

$$I_a = \frac{ig_s^2}{m_Q^2}\int\frac{d^Dk}{(2\pi)^D}\frac{\mathbf{p}\cdot\mathbf{p}' - (\mathbf{p}\cdot\mathbf{k})(\mathbf{p}'\cdot\mathbf{k})/\mathbf{k}^2}{k_0^2 - \mathbf{k}^2 + i\epsilon} \times\frac{1}{k_0 + i\epsilon}\frac{1}{k_0 + i\epsilon}. \quad (31)$$

After performing the contour integrating of $k_0 = |\mathbf{k}| - i\epsilon$,

[3]The Feynman rules are the same for the corresponding interaction terms in different regimes though their power counting may not be.

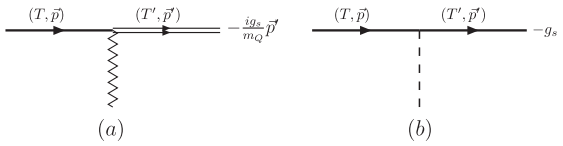

FIG. 7. NRQCD Feynman rules for a heavy-quark gluon vertex.

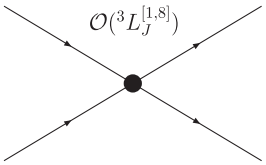

FIG. 8. NRQCD Feynman Diagram for LO matrix elements.

$$I_a = \frac{g_s^2}{2m_Q^2}\int\frac{d^{D-1}\mathbf{k}}{(2\pi)^{D-1}}\frac{\mathbf{p}\cdot\mathbf{p}' - (\mathbf{p}\cdot\mathbf{k})(\mathbf{p}'\cdot\mathbf{k})/\mathbf{k}^2}{|\mathbf{k}|^3}, \quad (32)$$

which is both infrared and ultraviolet divergent. In the dimension regularization scheme the result is

$$I_a = \frac{\alpha_s}{3\pi m_Q^2}\left(\frac{1}{\epsilon_{UV}} - \frac{1}{\epsilon}\right)\mathbf{p}\cdot\mathbf{p}'. \quad (33)$$

The integrals of (b–d) in Fig. 9 could be calculated in the same way:

$$I_{b-d} = \frac{\alpha_s}{3\pi m_Q^2}\left(\frac{1}{\epsilon_{UV}} - \frac{1}{\epsilon}\right)\mathbf{p}\cdot\mathbf{p}'. \quad (34)$$

The loop integral of diagram (e) in potential regime could be written down similarly:

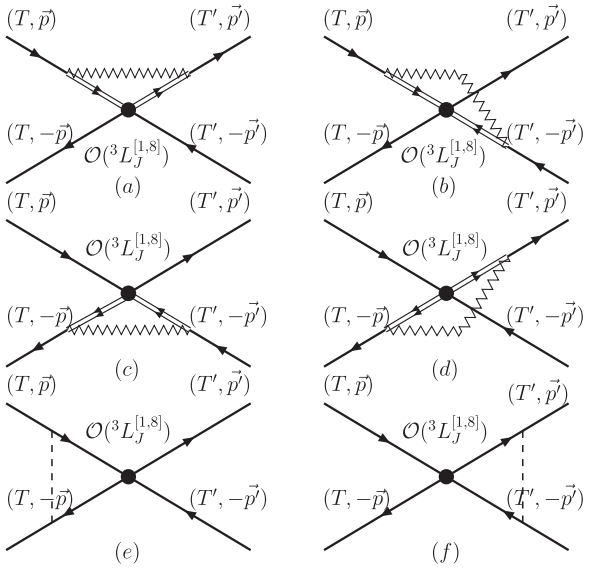

FIG. 9. NRQCD Feynman Diagrams for NLO matrix elements.

$$I_e = -ig_s^2 \int \frac{d^D k}{(2\pi)^D} \frac{1}{\mathbf{k}^2} \frac{1}{T + k_0 - \frac{(\mathbf{p}+\mathbf{k})^2}{2m_Q} + i\epsilon} \times \frac{1}{T - k_0 - \frac{(\mathbf{p}+\mathbf{k})^2}{2m_Q} + i\epsilon}, \tag{35}$$

where $T = \frac{|\mathbf{p}|^2}{2m_Q}$. When k_0 is integrated out:

$$I_e = g_s^2 m_Q \int \frac{d^{D-1}\mathbf{k}}{(2\pi)^{D-1}} \frac{1}{\mathbf{k}^2} \frac{1}{\mathbf{k}^2 + 2\mathbf{p}\cdot\mathbf{k} - i\epsilon}. \tag{36}$$

This could be done in D dimension directly. Regularize the Coulomb singularity by introducing $v = \frac{|\mathbf{p}|}{m_Q}$, then at v^{-1} order we have

$$I_e = \frac{\alpha_s \pi}{4v}\left(1 - \frac{i}{\pi}\left(\frac{1}{\epsilon} - \ln\left(\frac{m_Q^2 v^2}{\pi\mu^2}\right) - \gamma_E\right)\right). \tag{37}$$

The integral of diagram (f) has the same real part but with a plus sign before the virtual part.

The color structures for diagrams (a), (c) and (b), (d) and (e), (f) are obtained by the color decomposition listed in the first, second, and third line below, respectively:

$$\begin{aligned}
\sqrt{2}T^a T^b \otimes T^b \sqrt{2}T^a &= C_F \frac{1}{\sqrt{3}} \otimes \frac{1}{\sqrt{3}} + \frac{-2}{2N_c}\sqrt{2}T^c \otimes \sqrt{2}T^c, \\
\sqrt{2}T^a T^b \otimes \sqrt{2}T^a T^b &= C_F \frac{1}{\sqrt{3}} \otimes \frac{1}{\sqrt{3}} + \frac{N_c^2 - 2}{2N_c}\sqrt{2}T^c \otimes \sqrt{2}T^c, \\
T^b \sqrt{2}T^a T^b \otimes \sqrt{2}T^a &= \left(C_F - \frac{1}{2}C_A\right)\sqrt{2}T^c \otimes \sqrt{2}T^c.
\end{aligned} \tag{38}$$

Combining the integrals with the according color factors and summing them over, we obtain the NLO NRQCD corrections for the P-wave octet operator matrix elements, which are UV divergent and need to be renormalized:

$$\begin{aligned}
\langle \mathcal{O}^0({}^3P_J^{[8]})\rangle_{\mathrm{NLO}} = \Bigg\{ &\left(1 + \frac{\alpha_s \pi}{2v}\left(C_F - \frac{1}{2}C_A\right)\right)\sqrt{2}T^c \otimes \sqrt{2}T^c \\
&+ \frac{4\alpha_s}{3\pi m_Q^2}\left(\frac{1}{\epsilon_{UV}} - \frac{1}{\epsilon}\right)\Bigg[C_F \frac{1}{\sqrt{3}} \otimes \frac{1}{\sqrt{3}} \\
&+ B_F \sqrt{2}T^c \otimes \sqrt{2}T^c \Bigg]\mathbf{p}\cdot\mathbf{p}'\Bigg\}\langle \bar{\mathcal{O}}({}^3P_J)\rangle_{\mathrm{Born}},
\end{aligned} \tag{39}$$

where $\mathcal{O}({}^3P_J^{[8]}) = \bar{\mathcal{O}}({}^3P_J)\sqrt{2}T^a \otimes \sqrt{2}T^a$, $B_F = \frac{N_c^2 - 4}{4N_c}$ and the superscript "0" means the matrix elements of the bare operators. As expected, at NLO the P-wave octet operators are mixed with the D-wave singlet and octet ones, and with the help of Eq. (15), they could be reexpressed as

$$\begin{aligned}
\langle \mathcal{O}^0({}^3P_J^{[8]})\rangle_{\mathrm{NLO}} = &\left(1 + \frac{\alpha_s \pi}{2v}\left(C_F - \frac{1}{2}C_A\right)\right)\langle \mathcal{O}^0({}^3P_J^{[8]})\rangle_{\mathrm{Born}} \\
&+ \frac{4\alpha_s C_{J,J'}}{3\pi m_Q^2}\left(\frac{1}{\epsilon_{UV}} - \frac{1}{\epsilon}\right)(C_F\langle \mathcal{O}^0({}^3D_{J'}^{[1]})\rangle_{\mathrm{Born}} \\
&+ B_F\langle \mathcal{O}^0({}^3D_{J'}^{[8]})\rangle_{\mathrm{Born}}),
\end{aligned} \tag{40}$$

where $C_{J,J'}$ are defined in Eq. (16) and for $J' = 1, 2, 3$, $C_{0,J'} = \frac{(D-2)(D+1)}{2(D-1)^2}$, 0, 0; $C_{1,J'} = \frac{(D+1)}{4(D-1)}$, $\frac{3}{4}$, 0; $C_{2,J'} = \frac{(D-3)^2}{4(D-1)^2}$, $\frac{1}{4}$, 1. The P-wave operators are mixed with the D-wave operators at NLO in α_s. But the NLO NRQCD corrections of D-wave operators are related to the relativistic corrections of P-wave operators. Then at leading-order of v^2, the renormalization transformations of those operators in $\overline{MS}$ scheme are

$$\begin{aligned}
\begin{pmatrix} \mathcal{O}^0({}^3P_J^{[8]}) \\ \mathcal{O}^0({}^3D_{J'}^{[1]}) \end{pmatrix} &= \begin{pmatrix} 1 & C_{JJ'}^{[1]}\left(\frac{1}{\epsilon_{UV}} + \ln 4\pi - \gamma_E\right) \\ 0 & 1 \end{pmatrix} \\
&\times \begin{pmatrix} \mathcal{O}^R({}^3P_J^{[8]}) \\ \mathcal{O}^R({}^3D_{J'}^{[1]}) \end{pmatrix},
\end{aligned} \tag{41}$$

where $C_{JJ'}^{[1]} = C_{J,J'}\frac{4\alpha_s C_F}{3\pi m_Q^2}$. When the operators are mixed with each other, the renormalization constants Z's are not numbers but matrices. The D-wave octet operators are also dropped, for they do not appear in full QCD calculations. The matrix elements of the renormalized operators $\mathcal{O}^R({}^3P_J^{[8]})$ at NLO are now UV finite, but there are still $\frac{1}{\epsilon}$ poles in D-wave terms, Eq. (42), and Coulomb singularities, which will absorb the infrared and Coulomb divergences in full theory;

$$\begin{aligned}
\langle \mathcal{O}^R({}^3P_J^{[8]})\rangle_{\mathrm{NLO}} = &\left(1 + \frac{\alpha_s \pi}{2v}\left(C_F - \frac{1}{2}C_A\right)\right)\langle \mathcal{O}^R({}^3P_J^{[8]})\rangle_{\mathrm{Born}} \\
&+ \frac{4\alpha_s C_{J,J'}(\frac{\mu}{\mu_\Lambda})^{2\epsilon}}{3\pi m_Q^2}\left(-\frac{1}{\epsilon} - \ln 4\pi + \gamma_E\right) \\
&\times (C_F\langle \mathcal{O}^R({}^3D_{J'}^{[1]})\rangle_{\mathrm{Born}} \\
&+ B_F\langle \mathcal{O}^R({}^3D_{J'}^{[8]})\rangle_{\mathrm{Born}}),
\end{aligned} \tag{42}$$

where μ_Λ is the renormalization scale. The matrix elements of the S-wave octet operator at NLO could be computed in the same way:

$$\begin{aligned}
\langle \mathcal{O}^R({}^3S_1^{[8]})\rangle_{\mathrm{NLO}} = &\left(1 + \frac{\alpha_s \pi}{2v}\left(C_F - \frac{1}{2}C_A\right)\right)\langle \mathcal{O}^R({}^3S_1^{[8]})\rangle_{\mathrm{Born}} \\
&+ \frac{4\alpha_s(\frac{\mu}{\mu_\Lambda})^{2\epsilon}}{3\pi m_Q^2}\left(-\frac{1}{\epsilon} - \ln 4\pi + \gamma_E\right) \\
&\times (C_F\langle \mathcal{O}^R({}^3P_J^{[1]})\rangle_{\mathrm{Born}} \\
&+ B_F\langle \mathcal{O}^R({}^3P_J^{[8]})\rangle_{\mathrm{Born}}).
\end{aligned} \tag{43}$$

The matrix elements of the S-wave singlet operator and D-wave singlet operators at NLO do not need to be calculated, for their LO short-distance coefficients are already at $\mathcal{O}(\alpha_s^3)$.

Multiply the matrix elements with the short-distance coefficients, we obtain the NRQCD result at NLO in α_s:

$$(2\,\mathrm{Im}\mathcal{A}(^3S_1^{[1]}))_{\mathrm{NRQCD}} = \frac{2\,\mathrm{Im}f(^3S_1^{[1]})}{m_Q^2}\langle\mathcal{O}(^3S_1^{[1]})\rangle^R_{\mathrm{Born}}, \tag{44a}$$

$$(2\,\mathrm{Im}\mathcal{A}(^3S_1^{[8]}))_{\mathrm{NRQCD}} = \frac{2\,\mathrm{Im}f(^3S_1^{[8]})}{m_Q^2}\left(1+\frac{\alpha_s\pi}{2v}\left(C_F-\frac{1}{2}C_A\right)\right)\langle\mathcal{O}(^3S_1^{[8]})^R_{\mathrm{Born}}, \tag{44b}$$

$$(2\,\mathrm{Im}\mathcal{A}(^3P_0^{[8]}))_{\mathrm{NRQCD}} = \left\{\frac{2\,\mathrm{Im}f(^3P_0^{[8]})}{m_Q^4}\left(1+\frac{\alpha_s\pi}{2v}\left(C_F-\frac{1}{2}C_A\right)\right)-\frac{4\alpha_s B_F}{3\pi m_Q^4}\frac{2\,\mathrm{Im}f(^3S_1^{[8]})}{\epsilon}\left(\frac{4\pi\mu^2}{\mu_\Lambda^2}\right)^\epsilon\Gamma(1+\epsilon)\right\} \times\langle\mathcal{O}(^3P_0^{[8]})\rangle^R_{\mathrm{Born}}, \tag{44c}$$

$$(2\,\mathrm{Im}\mathcal{A}(^3P_1^{[8]}))_{\mathrm{NRQCD}} = \left\{\frac{2\,\mathrm{Im}f(^3P_1^{[8]})}{m_Q^4}\left(1+\frac{\alpha_s\pi}{2v}\left(C_F-\frac{1}{2}C_A\right)\right)-\frac{4\alpha_s B_F}{3\pi m_Q^4}\frac{2\,\mathrm{Im}f(^3S_1^{[8]})}{\epsilon}\left(\frac{4\pi\mu^2}{\mu_\Lambda^2}\right)^\epsilon\Gamma(1+\epsilon)\right\} \times\langle\mathcal{O}(^3P_1^{[8]})\rangle^R_{\mathrm{Born}}, \tag{44d}$$

$$(2\,\mathrm{Im}\mathcal{A}(^3P_2^{[8]}))_{\mathrm{NRQCD}} = \left\{\frac{2\,\mathrm{Im}f(^3P_2^{[8]})}{m_Q^4}\left(1+\frac{\alpha_s\pi}{2v}\left(C_F-\frac{1}{2}C_A\right)\right)-\frac{4\alpha_s B_F}{3\pi m_Q^4}\frac{2\,\mathrm{Im}f(^3S_1^{[8]})}{\epsilon}\left(\frac{4\pi\mu^2}{\mu_\Lambda^2}\right)^\epsilon\Gamma(1+\epsilon)\right\} \times\langle\mathcal{O}(^3P_2^{[8]})\rangle^R_{\mathrm{Born}}, \tag{44e}$$

$$(2\,\mathrm{Im}\mathcal{A}(^3D_1^{[1]}))_{\mathrm{NRQCD}} = \left\{\frac{2\,\mathrm{Im}f(^3D_1^{[1]})}{m_Q^6}-\sum_J\frac{4\alpha_s C_F C_{J,1}}{3\pi m_Q^6}\frac{2\,\mathrm{Im}f(^3P_J^{[8]})}{\epsilon}\left(\frac{4\pi\mu^2}{\mu_\Lambda^2}\right)^\epsilon\Gamma(1+\epsilon)\right\}\langle\mathcal{O}(^3D_1^{[1]})\rangle^R_{\mathrm{Born}}, \tag{44f}$$

$$(2\,\mathrm{Im}\mathcal{A}(^3D_2^{[1]}))_{\mathrm{NRQCD}} = \left\{\frac{2\,\mathrm{Im}f(^3D_2^{[1]})}{m_Q^6}-\sum_J\frac{4\alpha_s C_F C_{J,2}}{3\pi m_Q^6}\frac{2\,\mathrm{Im}f(^3P_J^{[8]})}{\epsilon}\left(\frac{4\pi\mu^2}{\mu_\Lambda^2}\right)^\epsilon\Gamma(1+\epsilon)\right\}\langle\mathcal{O}(^3D_2^{[1]})\rangle^R_{\mathrm{Born}}, \tag{44g}$$

$$(2\,\mathrm{Im}\mathcal{A}(^3D_3^{[1]}))_{\mathrm{NRQCD}} = \left(\frac{2\,\mathrm{Im}f(^3D_3^{[1]})}{m_Q^6}-\sum_J\frac{4\alpha_s C_F C_{J,3}}{3\pi m_Q^6}\frac{2\,\mathrm{Im}f(^3P_J^{[8]})}{\epsilon}\left(\frac{4\pi\mu^2}{\mu_\Lambda^2}\right)^\epsilon\Gamma(1+\epsilon)\right)\langle\mathcal{O}(^3D_3^{[1]})\rangle^R_{\mathrm{Born}}. \tag{44h}$$

Finally, matching the NRQCD results with full QCD results, we get infrared safe short-distance coefficients at $\mathcal{O}(\alpha_s^3)$:

$$2\,\mathrm{Im}f(^3S_1^{[1]}) = \frac{40\alpha_s^3(\pi^2-9)}{81}, \tag{45a}$$

$$2\,\mathrm{Im}f(^3S_1^{[8]}) = \frac{\alpha_s^2}{108}\left(36N_f\pi+\alpha_s\left(5(-657+67\pi^2)+N_f(642-20N_f-27\pi^2+72\ln 2)+72\beta_0 N_f\ln\frac{\mu}{2m_Q}\right)\right), \tag{45b}$$

$$2\,\mathrm{Im}f(^3P_0^{[8]}) = \frac{5\alpha_s^2}{1296}\left(648\pi+\alpha_s\left(9096-464N_f+63\pi^2+2520\ln 2+1296\beta_0\ln\frac{\mu}{2m_Q}+96N_f\ln\frac{2m_Q}{\mu_\Lambda}\right)\right), \tag{45c}$$

$$2\,\mathrm{Im}f(^3P_1^{[8]}) = \frac{5\alpha_s^3(4107-64N_f-414\pi^2+48N_f\ln\frac{2m_Q}{\mu_\Lambda})}{648}, \tag{45d}$$

$$2\,\mathrm{Im}f(^3P_2^{[8]}) = \frac{\alpha_s^2}{648}\left(432\pi+\alpha_s\left(12561-464N_f-774\pi^2+1008\ln 2+864\beta_0\ln\frac{\mu}{2m_Q}+240N_f\ln\frac{2m_Q}{\mu_\Lambda}\right)\right), \tag{45e}$$

$$2\,\mathrm{Im}f(^3D_1^{[1]}) = \frac{(321\pi^2-8032-29\,184\ln\frac{\mu_\Lambda}{2m_Q})\alpha_s^3}{5832}, \tag{45f}$$

$$2\,\mathrm{Im}f(^3D_2^{[1]}) = \frac{(425\pi^2-4816-384\ln\frac{\mu_\Lambda}{2m_Q})\alpha_s^3}{648}, \tag{45g}$$

$$2\,\mathrm{Im}f(^3D_3^{[1]}) = \frac{(529\pi^2-8688-5376\ln\frac{\mu_\Lambda}{2m_Q})\alpha_s^3}{2268}. \tag{45h}$$

The P- and D-wave short-distance coefficients are μ_Λ dependent, and their μ_Λ dependence can be canceled by the

renormalized operator μ_Λ dependence. The μ_Λ dependence of the renormalized operators could be derived out by finding the derivative of both sides of Eq. (41) with respect to μ_Λ:

$$\frac{d\mathcal{O}^R(^3P_J^{[8]})}{d\ln\mu_\Lambda} = \sum_{J'} \frac{C_{J,J'} 8\alpha_s C_F}{3\pi m_Q^2} \mathcal{O}^R(^3D_{J'}^{[1]}), \tag{46a}$$

$$\frac{d\mathcal{O}^R(^3S_1^{[8]})}{d\ln\mu_\Lambda} = \sum_{J} \frac{8\alpha_s B_F}{3\pi m_Q^2} \mathcal{O}^R(^3P_J^{[8]}), \tag{46b}$$

$$\frac{d\mathcal{O}^R(^3S_1^{[1]})}{d\ln\mu_\Lambda} = \sum_{J} \frac{1}{2N_C} \frac{8\alpha_s}{3\pi m_Q^2} \mathcal{O}^R(^3P_J^{[8]}). \tag{46c}$$

Remember, for bare quantities, $\frac{d\mathcal{O}^0(^3L_J^{[1,8]})}{d\mu_\Lambda} = 0$. For a phenomenological reason, we also give the μ_Λ dependence of $\mathcal{O}(^3S_1^{[1]})$, though we do not calculate its NLO NRQCD corrections. By solving the differential equations, all S- and P-wave operators' expectation values in $|H_{J'}\rangle$ states are related to that of the D-wave singlet operators:

$$\langle H_{J'}|\mathcal{O}^R(^3P_J^{[8]})(\mu_\Lambda)|H_{J'}\rangle = \langle H_{J'}|\mathcal{O}^R(^3P_J^{[8]})(\mu_{\Lambda_0})|H_{J'}\rangle + C_{J,J'}\frac{8C_F}{3m_Q^2\beta_0}\ln\frac{\alpha_s(\mu_{\Lambda_0})}{\alpha_s(\mu_\Lambda)}\langle H_{J'}|\mathcal{O}^R(^3D_{J'}^{[1]})|H_{J'}\rangle, \tag{47a}$$

$$\begin{aligned}\langle H_{J'}|\mathcal{O}^R(^3S_1^{[8]})(\mu_\Lambda)|H_{J'}\rangle = {}& \frac{C_F B_F}{2}\left(\frac{8}{3m_Q^2\beta_0}\ln\frac{\alpha_s(\mu_{\Lambda_0})}{\alpha_s(\mu_\Lambda)}\right)^2\langle H_{J'}|\mathcal{O}^R(^3D_{J'}^{[1]})|H_{J'}\rangle \\ & + \sum_J \frac{8B_F}{3m_Q^2\beta_0}\ln\frac{\alpha_s(\mu_{\Lambda_0})}{\alpha_s(\mu_\Lambda)}\langle H_{J'}|\mathcal{O}^R(^3P_J^{[8]})(\mu_{\Lambda_0})|H_{J'}\rangle + \langle H_{J'}|\mathcal{O}^R(^3S_1^{[8]})(\mu_{\Lambda_0})|H_{J'}\rangle,\end{aligned} \tag{47b}$$

$$\begin{aligned}\langle H_{J'}|\mathcal{O}^R(^3S_1^{[1]})(\mu_\Lambda)|H_{J'}\rangle = {}& \frac{C_F}{4N_C}\left(\frac{8}{3m_Q^2\beta_0}\ln\frac{\alpha_s(\mu_{\Lambda_0})}{\alpha_s(\mu_\Lambda)}\right)^2\langle H_{J'}|\mathcal{O}^R(^3D_{J'}^{[1]})|H_{J'}\rangle \\ & + \sum_J \frac{4}{3N_C m_Q^2\beta_0}\ln\frac{\alpha_s(\mu_{\Lambda_0})}{\alpha_s(\mu_\Lambda)}\langle H_{J'}|\mathcal{O}^R(^3P_J^{[8]})(\mu_{\Lambda_0})|H_{J'}\rangle + \langle H_{J'}|\mathcal{O}^R(^3S_1^{[1]})(\mu_{\Lambda_0})|H_{J'}\rangle.\end{aligned} \tag{47c}$$

In pNRQCD, the S-wave color-octet matrix elements for P-wave heavy quarkonium decays are also estimated through operator evolution equation [27,28]. And the relations between their results and ours are discussed in our previous work [29], which shows that the two methods are consistent with each other.

V. NUMERICAL RESULT AND DISCUSSION

A. ^3D_J decay into LH

For heavy-quark spin-symmetry, the long-distance matrix elements of D-wave four-fermion operators are equal to each other for different J, and relate to the second derivative of wave functions at the origin:

$$\begin{aligned}\frac{15|R''(0)|^2}{8\pi} &= \langle H_1|\mathcal{O}(^3D_1^{[1]})|H_1\rangle = \langle H_2|\mathcal{O}(^3D_2^{[1]})|H_2\rangle \\ &= \langle H_3|\mathcal{O}(^3D_3^{[1]})|H_3\rangle = H_D m_Q^6.\end{aligned} \tag{48}$$

The matrix elements of the P-wave octet operators and the S-wave singlet as well as octet operators in the corresponding J' states could be estimated through the resolution of operator evolution equations, Eq. (47). When μ_{Λ_0} and μ_Λ are separated widely enough, the evaluation terms will be much more important than the boundary terms labeled with μ_{Λ_0}. Here we set $\mu_{\Lambda_0} = m_Q v$, where $v^2 = 0.3$ for charmonium and $v^2 = 0.1$ for bottomonium, since the NRQCD perturbative calculations could only hold down to scale of order $m_Q v$:

$$\langle H_{J'}|\mathcal{O}^R(^3P_J^{[8]})(\mu_\Lambda)|H_{J'}\rangle = C_{J,J'}\frac{8C_F}{3\beta_0}\ln\frac{\alpha_s(\mu_{\Lambda_0})}{\alpha_s(\mu_\Lambda)}H_D m_Q^4, \tag{49a}$$

$$\langle H_{J'}|\mathcal{O}^R(^3S_1^{[8]})(\mu_\Lambda)|H_{J'}\rangle = \frac{C_F B_F}{2}\left(\frac{8}{3\beta_0}\ln\frac{\alpha_s(\mu_{\Lambda_0})}{\alpha_s(\mu_\Lambda)}\right)^2 H_D m_Q^2, \tag{49b}$$

$$\langle H_{J'}|\mathcal{O}^R(^3S_1^{[1]})(\mu_\Lambda)|H_{J'}\rangle = \frac{C_F}{4N_C}\left(\frac{8}{3\beta_0}\ln\frac{\alpha_s(\mu_{\Lambda_0})}{\alpha_s(\mu_\Lambda)}\right)^2 H_D m_Q^2. \tag{49c}$$

We also assume $\mu_\Lambda = \mu$, for the factorization scale μ_Λ in NRQCD also acts as the renormalization scale in operator renormalization. In the end, we come to the overall expressions for the LH decay widths of ^3D_J ($J = 1, 2, 3$) states to NLO in α_s at leading order of v^2:

$$\Gamma(^3D_1 \to \mathrm{LH}) = \left(-5.0\alpha_s^3\left(0.167 + \ln\frac{\mu}{2m_Q}\right) + \frac{\alpha_s^2(15.7 + \alpha_s(88.5 - 4.33N_f) + \alpha_s(10.0\beta_0 - 1.32N_f)\ln\frac{\mu}{2m_Q})\ln\frac{\bar{\alpha}_s}{\alpha_s}}{\beta_0} + \frac{1.32\alpha_s^2(1.57N_f - 0.278\alpha_s(N_f - 21.4)(N_f + 0.093) + 1.0N_f\alpha_s\beta_0\ln\frac{\mu}{2m_Q})\ln^2\frac{\bar{\alpha}_s}{\alpha_s}}{\beta_0^2}\right)H_D, \quad (50a)$$

$$\Gamma(^3D_2 \to \mathrm{LH}) = \left(-0.59\alpha_s^3\left(1.62 + \ln\frac{\mu}{2m_Q}\right) + \frac{\alpha_s^2(1.87 + \alpha_s(8.14 - 1.95N_f) + \alpha_s(1.19\beta_0 - 1.32N_f)\ln\frac{\mu}{2m_Q})\ln\frac{\bar{\alpha}_s}{\alpha_s}}{\beta_0} + \frac{1.32\alpha_s^2(1.57N_f - 0.278\alpha_s(N_f - 21.4)(N_f + 0.093) + 1.0N_f\alpha_s\beta_0\ln\frac{\mu}{2m_Q})\ln^2\frac{\bar{\alpha}_s}{\alpha_s}}{\beta_0^2}\right)H_D, \quad (50b)$$

$$\Gamma(^3D_3 \to \mathrm{LH}) = \left(-2.37\alpha_s^3\left(0.645 + \ln\frac{\mu}{2m_Q}\right) + \frac{\alpha_s^2(7.45 + \alpha_s(30.8 - 2.55N_f) + \alpha_s(4.74\beta_0 - 1.32N_f)\ln\frac{\mu}{2m_Q})\ln\frac{\bar{\alpha}_s}{\alpha_s}}{\beta_0} + \frac{1.32\alpha_s^2(1.57N_f - 0.278\alpha_s(N_f - 21.4)(N_f + 0.093) + 1.0N_f\alpha_s\beta_0\ln\frac{\mu}{2m_Q})\ln^2\frac{\bar{\alpha}_s}{\alpha_s}}{\beta_0^2}\right)H_D, \quad (50c)$$

where $\bar{\alpha}_s = \alpha_s(\mu_{\Lambda_0})$.

1. D-wave charmonium $\psi(1^3D_J)$ LH decay

Making a choice of $m_c = 1.5$ GeV, $\Lambda_{\mathrm{QCD}} = 390$ MeV, $H_{D1} = \frac{15|R_D''|^2}{8\pi m_c^6} = 0.786 \times 10^{-3}$ GeV [30], and $N_f = 3$ for charmonia, we obtain at $\mu = 2m_c$:

$$\Gamma(\psi(1^3D_J) \to \mathrm{LH}) = (435, 50, 172)\ \mathrm{keV} \quad \text{for } J = (1, 2, 3). \quad (51)$$

When $\mu = m_c$ and the other parameters are fixed, the results turn to be

$$\Gamma(\psi(1^3D_J) \to \mathrm{LH}) = (683, 42, 223)\ \mathrm{keV} \quad \text{for } J = (1, 2, 3). \quad (52)$$

And the μ dependence of the decay widths at $\mathcal{O}(\alpha_s^3)$ is shown in Fig. 10.

In the potential model, $\psi(1^3D_J)$ can only decay to $3g$ at α_s^3 order. The infrared divergences are regularized by ϵ_{be} the binding energy of the bound states. Accurate to ϵ_{be} order, potential model results [3] are

$$\Gamma_C(^3D_J \to \mathrm{LH}) = (160, 12, 68)\ \mathrm{keV}, \quad \text{for } J = (1, 2, 3). \quad (53)$$

If we reset their parameters the same as ours with $\alpha_s = \alpha_s(2m_c)$, $M = 2m_c = 3.0$ GeV, $|R_D''|^2 = 0.015$ GeV^7, the potential model predictions become

$$\Gamma_C(^3D_J \to \mathrm{LH}) = (240, 18, 102)\ \mathrm{keV}, \quad \text{for } J = (1, 2, 3). \quad (54)$$

It could be found that in the $c\bar{c}$ system the NRQCD predictions are about $2 \sim 3$ times larger than potential model results. In leading logarithm approximations [4], the ratios of the LH decay widths for $J = 1, 2, 3$ are $\Gamma(^3D_1):\Gamma(^3D_2):\Gamma(^3D_3) = \frac{76}{9}:1:4$. Including the non-negligible corrections to the leading logarithmic terms [3], the ratios turn to be: 40:3:17. And the relative ratios predicted by NRQCD at $\mu = 2m_c = 3.0$ GeV and $\mu = m_c = 1.5$ GeV are 43:5:17 and 34:2:11, respectively.

Much work has been done to predict the mass spectrum of $\psi(1^3D_J)$; some of the numerical results are collected in Refs. [31,32], and some theoretical work reviews may be found in Ref. [33] and references therein. All the predictions indicated that the masses of $\psi(1^3D_J)$ are all larger than the threshold of $D\bar{D}$ (about 3730 MeV), and the center of gravity of $1D$ states calculated in the Cornell potential [34] is 3815 MeV [35]. For its decay to open charm to be kinematically allowed, $\psi(1^3D_1)$ should not be a narrow state. It is believed that $\psi(3770)$ is primarily a 1^3D_1 state with a small admixture of the 2^3S_1 state [36,37], and the latest experimental average of its width is $\Gamma(\psi(3770)) = 27.3 \pm 1.0$ MeV [38]. But there is a long-standing puzzle

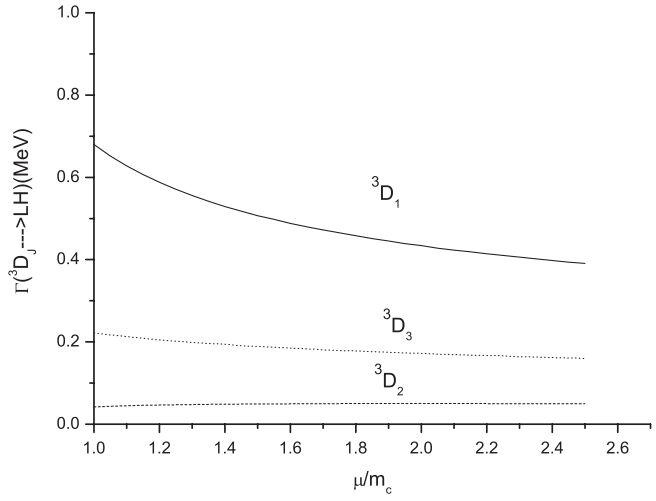

FIG. 10. Renormalization scale dependence of the decay widths of charmonium states 1^3D_J to LH at α_s^3 order.

in its non-$D\bar{D}$ decay that the $\psi(3770)$ decay is not saturated by the $D\bar{D}$ decay [39]. A detailed discussion about this problem could be found in our previous paper [40], and in this paper we will briefly review it in Sec. V B.

The remaining $J = 2$ and $J = 3$ states are both expected to be narrow with different reasons. $\psi(1^3D_2)$ is presumed to lie between the $D\bar{D}$ and $D\bar{D}^*$ thresholds [41] and is forbidden by parity to decay into two pseudoscalar D mesons. While narrowness of $\psi(1^3D_3)$ in contrast is due to suppression by the $D\bar{D}$ F-wave angular momentum barrier [31,41]. The principal decay modes of $\psi(1^3D_2)$ are radiative transition ($\psi(1^3D_2) \to \gamma\chi_{c1}, \gamma\chi_{c2}$), hadronic transition ($\psi(1^3D_2) \to J/\psi\pi\pi$), and LH decay. To $\psi(1^3D_3)$, these decay modes are also considerable since $\Gamma(\psi(1^3D_3) \to D\bar{D})$ is predicted to be only about 0.8 MeV [42], when its mass is 3868 MeV. And the decay widths predicted by the C^3 model [41,42] including the influence of open-charm channels are $\Gamma(\psi(1^3D_2) \to \gamma\chi_{c1}) = 212$ keV, $\Gamma(\psi(1^3D_J) \to \gamma\chi_{c2}) = (45, 286)$ keV, for $J = (2, 3)$ and $\Gamma(\psi(1^3D_3) \to D\bar{D}) = 0.82$ MeV at $m_{\psi(1^3D_2)} = 3831$ MeV and $m_{\psi(1^3D_3)} = 3868$ MeV. They also estimated $\Gamma(\psi(1^3D_J) \to J/\psi\pi\pi) = 68 \pm 15$ keV. Using the numerical values in Eq. (51), we then roughly predict that the branching ratios for the LH decay of $\psi(1^3D_J)$ are

$$\mathrm{Br}(\psi(1^3D_J) \to \mathrm{LH}) = 13.3\%, 13.3\%, \quad \text{for } J = (2, 3). \tag{55}$$

2. *D-wave bottomonium* $\Upsilon(n^3D_J)$ *LH decay*

Unlike charmonium, $\Upsilon(n^3D_J)$ (for $n = 1, 2$) are predicted to lie below the $B\bar{B}$ flavor threshold, and expected to be quite narrow, where n is the level number. Some predictions of $\Upsilon(1^3D_J)$ and $\Upsilon(2^3D_J)$ masses are reviewed in Ref. [43]. Taking $m_b = 4.6$ GeV, $\Lambda_{\mathrm{QCD}} = 340$ MeV, $N_f = 4$, $H_{D1} = \frac{15|R''_{1D}|^2}{8\pi m_b^6} = 0.401 \times 10^{-4}$ GeV for $1D$ states, and $H_{D2} = \frac{15|R''_{2D}|^2}{8\pi m_b^6} = 0.750 \times 10^{-4}$ GeV for $2D$ states [30], at $\mu = 2m_b$, we find

$$\Gamma(\Upsilon(1^3D_J) \to \mathrm{LH}) = (6.91, 0.75, 2.75)\ \mathrm{keV} \quad \text{for } J = (1, 2, 3), \tag{56a}$$

$$\Gamma(\Upsilon(2^3D_J) \to \mathrm{LH}) = (12.9, 1.40, 5.14)\ \mathrm{keV} \quad \text{for } J = (1, 2, 3). \tag{56b}$$

When $\mu = m_b$ and the other parameters are unchanged, our predictions turn to be

$$\Gamma(\Upsilon(1^3D_J) \to \mathrm{LH}) = (7.99, 0.60, 2.85)\ \mathrm{keV} \quad \text{for } J = (1, 2, 3), \tag{57a}$$

$$\Gamma(\Upsilon(2^3D_J) \to \mathrm{LH}) = (14.9, 1.21, 5.33)\ \mathrm{keV} \quad \text{for } J = (1, 2, 3). \tag{57b}$$

The μ dependence curves of $\Upsilon(1^3D_J)$ and $\Upsilon(2^3D_J)$ LH decay widths are similar, so only the $n = 1$ results are shown at $\mathcal{O}(\alpha_s^3)$ in Fig. 11 as an illustration.

In the potential model, Bélanger and Moxhay [4] found, for $J = (1, 2, 3)$, the leading logarithmic results are $\Gamma(\Upsilon(1^3D_J) \to ggg) = (2.2, 0.26, 1.1)$ keV, and a good approximation to the exact phase space integration given by Bergström and Ernström [3] brings a factor of $2 \sim 3$ enhancement, and their results are $\Gamma(\Upsilon(1^3D_J) \to ggg) = (6.3, 0.51, 2.7)$ keV, for $J = (1, 2, 3)$. If we normalize them using our inputs at $\mu = 2m_b$ and setting $M = 2m_b$, potential model estimations are then

$$\Gamma(\Upsilon(1^3D_J) \to \mathrm{LH}) = (5.4, 0.51, 2.3)\ \mathrm{keV} \quad \text{for } J = (1, 2, 3), \tag{58}$$

which, to some extent, are in agreement with our NRQCD numerical predictions with $\mu = 2m_b$. In the $\Upsilon(1D)$ case, it can be easily found out that the potential model results are dominated by the logarithmic terms. And numerically, the NRQCD results are mainly from the P-wave color-octet subprocess contributions. If we relate the logarithmic term $\ln(1/\epsilon)$ in Eqs. (20–22) of Ref. [3] to the evolution term $\ln\frac{\alpha_s(\mu_{\Lambda_0})}{\alpha_s(\mu_\Lambda)}$ in this paper by setting $\frac{\beta_0\alpha_s}{\pi}\ln(1/\epsilon) = \ln\frac{\alpha_s(\mu_{\Lambda_0})}{\alpha_s(\mu_\Lambda)}$, we find the logarithmic terms as well as the π^2 terms in the potential model results can be exactly reproduced within the NRQCD approach. This then provides an alternative way to relate the value of $\ln\frac{\alpha_s(\mu_{\Lambda_0})}{\alpha_s(\mu_\Lambda)}$ to the potential model estimation. Using the inputs $\langle r\rangle = 2.5\ \mathrm{GeV}^{-1}$ given in Ref. [3], $m_b = 4.6$ GeV, $\alpha_s = 0.18$, and $N_f = 4$, we get $\ln\frac{\alpha_s(\mu_{\Lambda_0})}{\alpha_s(\mu_\Lambda)} = 0.58$, which is consistent with the value we obtained by choosing $\mu_\Lambda = 2m_b$ and $\mu_{\Lambda_0} = m_b v_b$.

In Ref. [44], the branching ratios of some decay modes of $\Upsilon(1^3D_J)$ are summarized in Table IX, where $\Gamma(\Upsilon(1^3D_1) \to e^+e^-)$ was calculated in Ref. [45] and

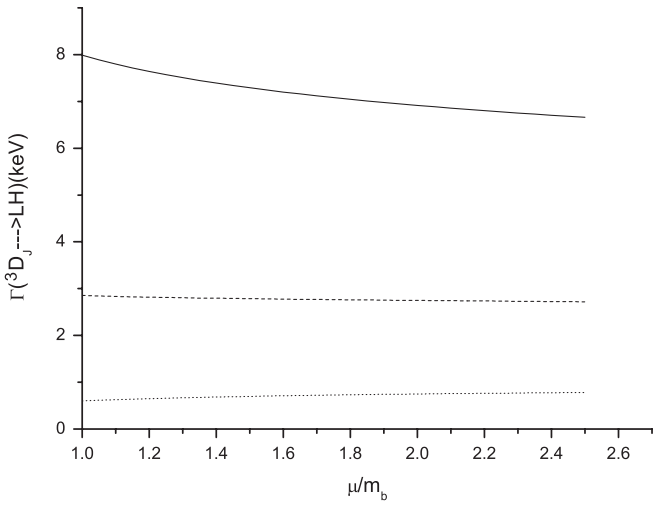

FIG. 11. Renormalization or factorization scale dependence of $\Gamma(\Upsilon(1^3D_J) \to \mathrm{LH})$ at α_s^3 order. The solid, dotted, and dashed lines are for $\Upsilon(1^3D_1)$, $\Upsilon(1^3D_2)$, and $\Upsilon(1^3D_3)$, respectively.

$\Gamma(\Upsilon(1^3D_J) \to \pi\pi)$ was obtained by Moxhay [46]. Since the LH decay widths of $\Upsilon(1^3D_J)$ are now calculated in the framework of NRQCD, we update the theoretical predictions for these ratios in Table IV, where the numerical results in Eq. (56a) are taken as estimations for LH decay widths of $\Upsilon(1^3D_J)$. In 2004, the CLEO Collaboration observed $\Upsilon(1D)$ in the four-photon cascade process $\Upsilon \to \gamma\chi_b(2P)$, $\chi_b(2P) \to \gamma\Upsilon(1D)$, $\Upsilon(1D) \to \gamma\chi_b(1P)$, $\chi_b(1P) \to \gamma\Upsilon(1S)$, followed by $\Upsilon(1S) \to l^+l^-$, and the branching ratio is $\mathcal{B}(\gamma\gamma\gamma\gamma l^+l^-)_{\Upsilon(1D)} = 2.5 \pm 0.5 \pm 0.5 \cdot 10^{-5}$ [47]. The signals are interpreted as predominantly coming from the production of $\Upsilon(1^3D_2)$. Small contributions of $\Upsilon(1^3D_1)$ and $\Upsilon(1^3D_3)$ can not be ruled out. In the near future, with more accumulated data, all the spin-triplet $\Upsilon(1^3D_J)$ states may be identified. Unfortunately, the D-wave bottomonium LH decays could not provide a good probe to find out whether NRQCD is prior to the potential model to describe the bottomonium system, for the difference between the two theoretical predictions is small, unless a very precise measurement is made.

For the $n = 2$ states, no experimental evidence has been observed until now. To make a theoretical comparison for $\Gamma(\Upsilon(2^3D_J) \to \text{LH})$, the numerical potential model predictions are needed.

B. LH decay of $\psi(3770)$

Recently, BES reported [48–50] that the branching ratio of the non-$D\bar{D}$ decay of $\psi(3770)$ is about 15%. While the corresponding data of CLEO [51] imply zero. The total width $\Gamma(\psi(3770))$ is 23.0 ± 2.7 MeV [52],[4] and the hadronic and E1 radiative transitions contribute about only 350–400 keV and 1.5–1.8% to the decay width and the branching ratio of non-$D\bar{D}$ decay mode, respectively. To clarify this puzzle, the annihilation decay of $\psi(3770)$, i.e. $\psi(3770) \to \text{LH}$, is considered in our previous paper [40], where $\psi(3770)$ is taken as a D-wave dominated state with a small admixture of the $2S$ state. We found when the annihilation decay is included, $\Gamma(\psi(3770) \to \text{non-}D\bar{D})$ is $1.15 \sim 1.20$ MeV, corresponding to branching ratio of about 5%.

In the above sections, the short-distance coefficients and long-distance matrix elements of $\psi(1^3D_1)$ have been given in detail. Now, we show how to get the S-D mixing term. The typical Feynman diagram for interference between the color-singlet $^3S_1$ and $^3D_1$ is shown in Fig. 12. The interference between other Fock states of S-wave and D-wave are suppressed by α_s or v^2. For example, the interference between two P-wave octet states is of relative v^2 order. And the S-wave singlet interference is of relative α_s^2 order, since there are at least two additional gluons in the S-wave Fock state of $^3D_1^{[1]}$. In full QCD, the square of the D-wave amplitude is logarithm divergent in phase space integration, and that of S-wave amplitude is finite, therefore, the combination of them will be finite. Then the short-distance part in Eq. (59) could be calculated in 4 dimension:

$$2\,\mathrm{Im}\bar{\mathcal{A}}((Q\bar{Q})^{[1]}_{^3D_1} \to (Q\bar{Q})^{[1]}_{^3S_1}) = \frac{1}{3}\int \mathrm{Re}\Big[\sum |\bar{\mathcal{M}}((Q\bar{Q})^{[1]}_{^3D_1} \to \mathrm{LH})\bar{\mathcal{M}}^*((Q\bar{Q})^{[1]}_{^3S_1} \to \mathrm{LH})\Big] d\Phi. \tag{59}$$

Taking into account the corresponding long-distance part, we then obtain the final expression for the mixing term in Ref. [40]:

$$\langle 1^3D_1|\mathrm{LH}\rangle\langle \mathrm{LH}|2^3S_1\rangle = \frac{5\alpha_s^3(-240 + 71\pi^2)}{324m_c^4}\frac{R_{2S}(0)}{\sqrt{4\pi}} \times \sqrt{\frac{1}{8\pi}}R''_{1D}(0). \tag{60}$$

TABLE IV. Summary of the partial widths and branching ratios (B) for spin-triplet $b\bar{b}$ D-wave states, where $\Gamma(\Upsilon(1^3D_J) \to \text{LH})$ are predicted by us in Eq. (56a), and the decay widths of the other modes are the same as those in Table IX of Ref. [44].

Level	Final state	Width (keV)	B(%)
$\Upsilon(1^3D_1)$	$\gamma + \chi_b(1^3P_0)$	21.4	53.1
	$\gamma + \chi_b(1^3P_1)$	11.3	28.1
	$\gamma + \chi_b(1^3P_2)$	0.58	1.44
	LH	6.91	17.2
	$\Upsilon\pi\pi$	0.07	0.17
	e^+e^-	0.0015	0.0037
	all	40.3	100
$\Upsilon(1^3D_2)$	$\gamma + \chi_b(1^3P_1)$	22.0	77.1
	$\gamma + \chi_b(1^3P_2)$	5.7	20.0
	LH	0.75	2.63
	$\Upsilon\pi\pi$	0.07	0.25
	all	28.5	100
$\Upsilon(1^3D_3)$	$\gamma + \chi_b(1^3P_2)$	24.3	89.6
	LH	2.75	10.1
	$\Upsilon\pi\pi$	0.07	0.26
	all	27.1	100

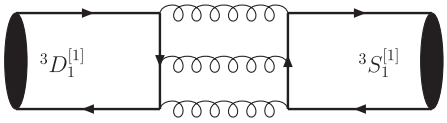

FIG. 12. QCD Feynman Diagram for the S-D mixing term.

VI. SUMMARY

In this paper, in the framework of NRQCD we study the light hadron (LH) decays of the spin-triplet ($S = 1$) D-wave heavy quarkonia. For completeness, the short-

[4]In this subsection, we still cite PDG06 data, to be in consistent with our analysis in Ref. [40]

distance coefficients of all Fock states in the ${}^3D_J$ ($J = 1, 2, 3$) quarkonia including D-wave color-singlet, P-wave color-octet, and S-wave color-singlet and color-octet are calculated perturbatively at α_s^3 order. The infrared divergences in D-wave singlet states are absorbed by the P-wave color-octet matrix elements. The operator evolution equations of the four-fermion operators are also derived and are used to estimate the numerical values of the long-distance matrix elements. We find that for the $c\bar{c}$ system, the LH decay widths of $\psi(1^3D_J)$ predicted by NRQCD is about $2 \sim 3$ times larger than the phenomenological potential model results, while for the $b\bar{b}$ system the two theoretical estimations of $\Gamma(\Upsilon(1^3D_J) \to \mathrm{LH})$ are in coincidence with each other.

ACKNOWLEDGMENTS

This work was supported by the National Natural Science Foundation of China (No 10675003, No 10721063) and the Ministry of Science and Technology of China (No 2009CB825200). Zhi-Guo He is currently supported by the CPAN08-PD14 contract of the CSD2007-00042 Consolider-Ingenio 2010 program, and by the FPA2007-66665-C02-01/ project (Spain).

[1] R. Barbieri, R. Gatto, and E. Remiddi, Phys. Lett. **61B**, 465 (1976); R. Barbieri, M. Caffo, and E. Remiddi, Nucl. Phys. **B162**, 220 (1980).
[2] R. Barbieri, M. Caffo, R. Gatto, and E. Remiddi, Phys. Lett. **95B**, 93 (1980); Nucl. Phys. **B192**, 61 (1981).
[3] L. Bergstrom and P. Ernstrom, Phys. Lett. B **267**, 111 (1991).
[4] G. Belanger and P. Moxhay, Phys. Lett. B **199**, 575 (1987).
[5] G. T. Bodwin, E. Braaten, and G. P. Lepage, Phys. Rev. D **46**, R1914 (1992).
[6] G. T. Bodwin, E. Braaten, and G. P. Lepage, Phys. Rev. D **51**, 1125 (1995); **55**, 5853(E) (1997).
[7] H. w. Huang and K. t. Chao, Phys. Rev. D **54**, 3065 (1996); **56**, 7472(E) (1997); **60**, 079901(E) (1999).
[8] Han-Wen Huang and Kuang-Ta Chao, Phys. Rev. D **54**, 6850 (1996); **56**, 1821(E) (1997).
[9] A. Petrelli, Phys. Lett. B **380**, 159 (1996).
[10] A. Petrelli, M. Cacciari, M. Greco, F. Maltoni, and M. L. Mangano, Nucl. Phys. **B514**, 245 (1998).
[11] Han-Wen Huang and Kuang-Ta Chao, Phys. Rev. D **55**, 244 (1997).
[12] N. Brambilla *et al.* (Quarkonium Working Group), arXiv: hep-ph/0412158.
[13] N. Brambilla, E. Mereghetti, and A. Vairo, J. High Energy Phys. 08 (2006) 039; Phys. Rev. D **79**, 074002 (2009).
[14] J. H. Kühn, J. Kaplan, and E. G. Safiani, Nucl. Phys. **B157**, 125 (1979); B. Guberina, J. H. Kühn, R. D. Peccei, and R. Rückl, Nucl. Phys. **B174**, 317 (1980).
[15] G. T. Bodwin and A. Petrelli, Phys. Rev. D **66**, 094011 (2002).
[16] S. Tani, Prog. Theor. Phys. **6**, 267 (1951); L. L. Foldy and S. A. Wouthuysen, Phys. Rev. **78**, 29 (1950).
[17] M. Klasen, B. A. Kniehl, L. N. Mihaila, and M. Steinhauser, Nucl. Phys. **B713**, 487 (2005); Phys. Rev. D **71**, 014016 (2005).
[18] P. Labelle, Phys. Rev. D **58**, 093013 (1998).
[19] M. Luke and A. V. Manohar, Phys. Rev. D **55**, 4129 (1997).
[20] B. Grinstein and I. Z. Rothstein, Phys. Rev. D **57**, 78 (1998).
[21] M. Luke and M. J. Savage, Phys. Rev. D **57**, 413 (1998).
[22] A. Pineda and J. Soto, Nucl. Phys. B, Proc. Suppl. **64**, 428 (1998).
[23] M. Beneke and V. A. Smirnov, Nucl. Phys. **B522**, 321 (1998); Report No. CERN-TH-97-315.
[24] A. Pineda and J. Soto, Phys. Lett. B **420**, 391 (1998); Phys. Rev. D **59**, 016005 (1998).
[25] H. W. Grießhammer, Phys. Rev. D **58**, 094027 (1998); arXiv:hep-ph/9804251.
[26] N. Brambilla, A. Pineda, J. Soto, and A. Vairo, Nucl. Phys. **B566**, 275 (2000); Phys. Rev. D **63**, 014023 (2000).
[27] N. Brambilla, D. Eiras, A. Pineda, J. Soto, and A. Vairo, Phys. Rev. Lett. **88**, 012003 (2001).
[28] N. Brambilla, D. Eiras, A. Pineda, J. Soto, and A. Vairo, Phys. Rev. D **67**, 034018 (2003).
[29] Y. Fan, Z. G. He, Y. Q. Ma, and K. T. Chao, Phys. Rev. D **80**, 014001 (2009).
[30] E. J. Eichten and C. Quigg, Phys. Rev. D **52**, 1726 (1995).
[31] T. Barnes and S. Godfrey, Phys. Rev. D **69**, 054008 (2004).
[32] E. S. Swanson, Phys. Rep. **429**, 243 (2006).
[33] E. Eichten, S. Godfrey, H. Mahlke, and J. L. Rosner, Rev. Mod. Phys. **80**, 1161 (2008).
[34] E. Eichten, K. Gottfried, T. Kinoshita, K. D. Lane, and T. M. Yan, Phys. Rev. D **17**, 3090 (1978); **21**, 313(E) (1980).
[35] E. J. Eichten, K. Lane, and C. Quigg, Phys. Rev. Lett. **89**, 162002 (2002).
[36] Y. B. Ding, D. H. Qin, and K. T. Chao, Phys. Rev. D **44**, 3562 (1991).
[37] J. L. Rosner, Phys. Rev. D **64**, 094002 (2001).
[38] C. Amsler *et al.* (Particle Data Group), Phys. Lett. B **667**, 1 (2008).
[39] G. Rong, D. H. Zhang, and J. C. Chen, arXiv:hep-ex/ 0506051.
[40] Z. G. He, Y. Fan, and K. T. Chao, Phys. Rev. Lett. **101**, 112001 (2008).
[41] E. J. Eichten, K. Lane, and C. Quigg, Phys. Rev. D **69**, 094019 (2004).
[42] E. J. Eichten, K. Lane, and C. Quigg, Phys. Rev. D **73**, 014014 (2006); **73**, 079903(E) (2006).
[43] S. Godfrey and J. L. Rosner, Phys. Rev. D **64**, 097501 (2001); **66**, 059902(E) (2002).
[44] W. Kwong and J. L. Rosner, Phys. Rev. D **38**, 279 (1988).

[45] P. Moxhay and J. L. Rosner, Phys. Rev. D **28**, 1132 (1983).
[46] P. Moxhay, Phys. Rev. D **37**, 2557 (1988).
[47] G. Bonvicini *et al.* (CLEO Collaboration), Phys. Rev. D **70**, 032001 (2004).
[48] M. Ablikim *et al.* (BES Collaboration), Phys. Lett. B **641**, 145 (2006).
[49] M. Ablikim *et al.* (BES Collaboration), Phys. Rev. Lett. **97**, 121801 (2006).
[50] M. Ablikim *et al.* (BES Collaboration), Phys. Rev. D **76**, 122002 (2007).
[51] D. Besson *et al.* (CLEO Collaboration), Phys. Rev. Lett. **96**, 092002 (2006).
[52] W. M. Yao *et al.* (Particle Data Group), J. Phys. G **33**, 1 (2006).